

1 **Running Title: SVR9 regulates chloroplast and leaf development**

2

3 Corresponding author:

4 Fei Yu

5 State Key Laboratory of Crop Stress Biology for Arid Areas and College of Life Sciences,

6 Northwest A&F University, Yangling, Shaanxi 712100, China

7

8 Tel (Fax): +86-29-87091935

9 E-mail: flyfeiyu@gmail.com

10

11 **Research Area: Genes, Development and Evolution**

12

13

14

15 **Title:** Chloroplast translation initiation factors regulate leaf variegation and
16 development

17

18 Mengdi Zheng^{1*}, Xiayan Liu^{1*}, Shuang Liang¹, Shiyong Fu¹, Yafei Qi¹, Jun Zhao¹, Jingxia
19 Shao¹, Lijun An¹, Fei Yu^{1§}

20

21 ¹ State Key Laboratory of Crop Stress Biology for Arid Areas and College of Life Sciences,
22 Northwest A&F University, Yangling, Shaanxi 712100, People's Republic of China

23

24 *These authors contributed equally to this article.

25

26 **One-sentence summary**

27 SVR9 and its homologue SVR9L1 encode functionally redundant chloroplast translation initiation
28 factors essential for chloroplast and leaf development in Arabidopsis

29

30

31

32 **Footnotes**

33 This work was supported by grants from the National Natural Science Foundation of China
34 (31170219 and 31570267 to F.Y., 31300988 to Y.Q. and 31400216 to J.Z.).

35

36 Corresponding author: Fei Yu, Email: flyfeiyu@gmail.com

37

38 **Author contributions**

39 F.Y. conceived and designed research plans; X.L. supervised the experiments; M.Z., S.L. and
40 S.F. performed experiments; M.Z., Y.Q., and J.Z. analyzed the data; L.A. and J.S. provided
41 technical assistance; F.Y. and X.L. wrote the article with contributions from all the authors.

42

43

44 **ABSTRACT**

45 Chloroplast development requires the coordinated expressions of nuclear and chloroplast
46 genomes, and both anterograde and retrograde signals exist and work together to facilitate this
47 coordination. We have utilized the *Arabidopsis yellow variegated* (*var2*) mutant as a tool to
48 dissect the genetic regulatory network of chloroplast development. Here, we report the
49 isolation of a new *var2* genetic suppressor locus, *SUPPRESSOR OF VARIEGATION9* (*SVR9*).
50 *SVR9* encodes a chloroplast-localized prokaryotic type translation initiation factor IF3. *svr9-1*
51 mutant can be fully rescued by the *Escherichia coli* IF3 infC, suggesting that *SVR9* functions
52 as a *bona fide* IF3 in the chloroplast. Genetic and molecular evidence indicate that *SVR9* and
53 its close homologue *SVR9-LIKE1* (*SVR9L1*) are functionally interchangeable and their
54 combined activities are essential for chloroplast development and plant survival. Interestingly,
55 we found that *SVR9* and *SVR9L1* are also involved in normal leaf development.
56 Abnormalities in leaf anatomy, cotyledon venation patterns and leaf margin development
57 were identified in *svr9-1* and mutants that are homozygous for *svr9-1* and heterozygous for
58 *svr9l1-1* (*svr9-1 svr9l1-1/+*). Meanwhile, as indicated by the auxin response reporter
59 *DR5:GUS*, auxin homeostasis was disturbed in *svr9-1*, *svr9-1 svr9l1-1/+* and plants treated
60 with inhibitors of chloroplast translation. Genetic analysis established that *SVR9/SVR9L1*-
61 mediated leaf margin development is dependent on *CUP-SHAPED COTYLEDON2* activities
62 and is independent of their roles in chloroplast development. Together, our findings provide
63 direct evidence that chloroplast IF3s are essential for chloroplast development and they can
64 also regulate leaf development.

65

66

67 **Introduction**

68 One of the most remarkable achievements in nature is the evolution of the semi-
69 autonomous organelles including chloroplasts and mitochondria in eukaryotic cells via
70 endosymbiosis (Dyall et al., 2004; Jensen and Leister, 2014). Current-day chloroplasts are
71 estimated to contain ~3000 proteins, similar to their cyanobacterial ancestors (Leister, 2003).
72 However, during the endosymbiotic process, the vast majority of genes encoding chloroplast
73 proteins has been transferred to the nucleus and became part of the nuclear genome, and
74 consequently higher plants have evolved regulatory pathways that exert control over these
75 nuclear genes for chloroplast proteins (Woodson and Chory, 2008). The fine coordination
76 between the nucleus and the chloroplast has been fulfilled via two-way communications from
77 the nucleus to the chloroplast (anterograde) and also from the chloroplast to the nucleus
78 (retrograde) (Nott et al., 2006; Woodson and Chory, 2012; Chi and Zhang, 2013).

79 Much of what we know regarding retrograde signaling stemmed from the regulation of
80 the expressions of nuclear genes for chloroplast proteins by the functional and developmental
81 states of the chloroplast. In wild type *Arabidopsis* seedlings, carotenoid biosynthesis inhibitor
82 norflurazon (NF) can induce photobleaching of the chloroplast and trigger the massive down
83 regulation of nuclear genes for chloroplast proteins such as *CHLOROPHYLL A/B BINDING*
84 *PROTEIN (CAB)* (Nott et al., 2006; Chi and Zhang, 2013). Taking advantage of this NF-
85 triggered retrograde response, a series of *genomes uncoupled (gun)* mutants that retained *CAB*
86 expressions upon NF treatment have been identified (Susek et al., 1993; Koussevitzky et al.,
87 2007). Based on the *GUN* and other work, the chlorophyll biosynthetic precursor, Mg-
88 protoporphyrin IX (Mg-protoIX), has been shown as one molecule that potentially serves as
89 the signal molecule in the NF-triggered retrograde signaling, although there are reports
90 arguing against this notion (Mochizuki et al., 2008; Moulin et al., 2008). AP2 type
91 transcription factor ABA INSENSITIVE4 (*ABI4*) has been identified as a nuclear
92 transcription repressor that executes retrograde signaling downstream of chloroplast *GUNs*
93 (Koussevitzky et al., 2007). Additional retrograde signals and signaling components have also
94 been identified. A screen with low concentration of NF and light intensity has identified
95 additional *happy on norflurazon (hon)* mutants (Saini et al., 2011). A chloroplast envelope
96 anchored plant homeodomain transcription factor PTM may be involved in signal
97 transduction from the plastid to the nucleus and PTM was shown to be able to bind the
98 promoter of *ABI4* and activate its expression (Sun et al., 2011). The physiological states of the
99 chloroplast can also trigger signaling to the nucleus (Wilson et al., 2009; Leister, 2012). For
100 example, the redox state of the photosynthetic electron transfer chain has long been thought
101 as a generator of chloroplast-derived signals (Pesaresi et al., 2009; Kindgren et al., 2012).
102 Reactive oxygen species such as singlet oxygen generated from chloroplasts are also able to
103 trigger nuclear gene expression responses, via an EXECUTER1 and 2-mediated pathway

104 (Wagner et al., 2004; Lee et al., 2007; Galvez-Valdivieso and Mullineaux, 2010; Ramel et al.,
105 2012). Recently, a plastid isoprenoid biosynthetic intermediate, methylerythritol phosphate
106 (MEcPP), was shown to be a new retrograde signal and able to trigger the expression of stress
107 related nuclear genes such as *HYDROPEROXIDE LYASE (HPL)* (Xiao et al., 2012). Plastid
108 gene expression (PGE) has also been proposed as a source of retrograde signals (Gray et al.,
109 2003). Chloroplast translation inhibitors such as lincomycin could trigger the down-regulation
110 of photosynthesis associated nuclear genes, which may be part of the broader PGE-mediated
111 retrograde pathway (Pesaresi et al., 2006).

112 Besides these retrograde signaling pathways that often use the expressions of nuclear
113 genes for chloroplast proteins as the readout, there is also evidence suggesting other modes of
114 retrograde regulation, for example, the influence on overall plant growth and development by
115 the functional and developmental states of the chloroplast (Hricová et al., 2006; Fleischmann
116 et al., 2011; Tiller and Bock; 2014). In the *Arabidopsis thaliana immutans* mutant and the
117 tomato *ghost* mutant, both defective in the plastid alternative oxidase and displaying
118 distinctive green-white leaf variegation phenotypes, there are conspicuous leaf mesophyll cell
119 developmental defects in white leaf sectors (Josse et al., 2000; Aluru et al., 2001). Some
120 *Arabidopsis* albino mutants such as *pale cress* and *clal* were also shown to have leaves that
121 lack the characteristic palisade tissue (Reiter et al., 1994; Mandel et al., 1996). In contrast to
122 the rapid progressing of the overall field of plastid retrograde signaling, our understanding of
123 the regulation of plant and leaf development by the developmental and functional states of the
124 chloroplast has remained descriptive.

125 We have used the *Arabidopsis* leaf variegation mutant *var2* as a tool to probe the genetic
126 regulation of chloroplast development (Liu et al., 2010a; 2013; Qi et al., 2015). In this work,
127 we report the identification of a *var2* genetic suppressor gene *SUPPRESSOR OF*
128 *VARIATION9 (SVR9)*. Molecular cloning and functional complementation tests established
129 that SVR9 and its homologue SVR9-Like1 (SVR9L1) act redundantly as chloroplast
130 translation initiation factor IF3. Down-regulation of chloroplast IF3s' activities not only
131 caused chloroplast development defects, but also led to a series of leaf developmental
132 abnormalities including more serrated leaf margin, disorganized mesophyll cells and altered
133 cotyledon venation patterns. We further demonstrated that auxin homeostasis is disturbed in
134 mutants defective in chloroplast IF3s or in plants treated with chloroplast translation
135 inhibitors. Genetic evidence suggests that the NAC family transcription factor CUP-SHAPED
136 COTYLEDON2 (CUC2) is involved in the chloroplast IF3-mediated leaf margin
137 development (Nikovics et al., 2006). Our results suggest that chloroplast translation initiation
138 factors SVR9 and SVR9L1 are required not only for chloroplast development and *var2*-
139 mediated leaf variegation, but also are involved in the coordination of leaf and chloroplast
140 development.

141

142 **Results**

143 **The isolation and cloning of an extragenic *var2* suppressor locus *SVR9***

144 We have isolated and characterized genetic suppressors of the *var2* leaf variegation
145 mutant through an activation tagging screen in the *var2-5* mutant background (Liu et al.,
146 2010a; Putarjunan et al., 2013). Here we report the isolation of a new *var2-5* suppressor
147 mutant designated *092-004* (Fig. 1A). Following our naming system, the suppressor locus in
148 *092-004* was named *SUPPRESSOR OF VARIEGATION9 (SVR9)*, and the genotype of *092-*
149 *004* was *var2-5 svr9-1* and the suppressor single mutant was *svr9-1*. Phenotypically, *svr9-1*
150 showed a distinctive virescent phenotype, i.e., young and emerging leaf tissues displayed
151 pronounced chlorosis while these yellow tissues gradually turned green as mutant leaves
152 matured (Fig. 1A). Consistent with the virescent appearance, chlorophylls accumulated at
153 lower levels in young and emerging tissues, but increased in mature tissues in *svr9-1* and *092-*
154 *004* (Fig. 1B). The suppression of *var2* leaf variegation by *svr9-1* was not allele specific as
155 *svr9-1* can suppress a stronger *var2* allele, *var2-4* (Fig. 1C and 1D).

156 Initial co-segregation analyses judged by herbicide Basta resistance indicated that *svr9-1*
157 was likely linked with T-DNA, but we were not able to identify the T-DNA insertion site via
158 various techniques. We thus utilized a map-based cloning procedure to identify *SVR9* (Fig. 2).
159 Bulk segregant analysis and subsequent fine mapping narrowed *SVR9* to a ~415 kb region
160 on chromosome 2 (Fig. 2A). Based on the *svr9-1* phenotype, we reasoned that *SVR9* likely
161 codes for a chloroplast-localized protein. DNA sequences of potential nuclear genes for
162 chloroplast proteins in the interval were examined. Surprisingly, PCRs failed to amplify
163 genomic regions around intron 4 of At2g24060 in *svr9-1*, suggesting At2g24060 genomic
164 sequences may be altered in *svr9-1* (Fig. 2B). Consistent with an abnormality at genomic
165 DNA level, At2g24060 transcripts were not detected in *svr9-1* (Fig. 2C). These results
166 indicated that At2g24060 is disrupted in *svr9-1*.

167

168 ***SVR9* encodes a chloroplast translation initiation factor IF3**

169 To confirm that the virescent phenotype of *svr9-1* and the suppression of *var2-5* were
170 indeed due to a potential disruption of At2g24060, we carried out complementation tests.
171 Independent transgenic lines over-expressing At2g24060 under the 35S promoter were able to
172 reverse the virescent phenotype of *svr9-1* and restore the leaf variegation phenotype in *092-*
173 *004*, thus confirming that At2g24060 is *SVR9* (Fig. 3A).

174 *SVR9/At2g24060* was annotated to encode a putative chloroplast protein of 312 amino
175 acids. *SVR9* shows high homologies with translation initiation factor 3 (IF3) proteins in
176 prokaryotes (Supplemental Fig. S1). To test whether the virescent phenotype of *svr9-1* was
177 indeed caused by the lack of a chloroplast IF3, we carried out functional complementation

178 tests using the *Escherichia coli* IF3 protein infC (Sacerdot et al., 1982). First, we established
179 that the putative chloroplast transit peptide of SVR9 (cTP_{SVR9}, N-terminal 1-71 amino acid
180 residues of SVR9) was sufficient to guide GFP into the chloroplast (Supplemental Fig. S2).
181 Then a binary vector containing a chimeric gene with the cTP_{SVR9} fused at the N-terminus of
182 *E. coli* infC under the control of the 35S promoter was generated (*P*_{35S}:cTP_{SVR9}-infC) and
183 transformed into *svr9-1*. Independent transgenic plants showed green leaf coloration,
184 indicating that cTP_{SVR9}-infC can functionally replace SVR9 (Fig. 3B). Moreover, when
185 *P*_{35S}:cTP_{SVR9}-infC was introduced into 092-004, transgenic plants showed leaf variegation
186 phenotype resembled that of *var2-5*, suggesting also a functional complementation (Fig. 3B).
187 These results indicate that *E. coli* infC can substitute for SVR9 and the phenotype of *svr9-1*
188 and the suppression of *var2-5* leaf variegation by *svr9-1* were caused by the lack of a
189 chloroplast translation initiation factor IF3.

190 Phylogenetic analysis of SVR9-like proteins in various photosynthetic organisms showed
191 that higher plant chloroplasts often contain more than one IF3 coding genes (Supplemental
192 Fig. S3). In *Arabidopsis*, two other genes, At4g30690 and At1g34360, also potentially code
193 for prokaryotic IF3-like proteins (Fig. 4A; Nesbit et al., 2015). Of the three genes, SVR9 and
194 At4g30690 code for putative chloroplast proteins and share the same gene structures, and
195 ~78% identities in amino acid sequences (Fig. 4A; Supplemental Figs. S1 and S3). We thus
196 named At4g30690 as SVR9-LIKE1 (SVR9L1). In contrast, At1g34360 codes for a
197 mitochondrial protein and its gene structure was different from that of SVR9 or At4g30690
198 (Fig. 4A; Nesbit et al., 2015). To confirm the chloroplast localizations of SVR9 and SVR9L1,
199 constructs expressing C-terminal GFP fusion proteins SVR9-GFP and SVR9L1-GFP were
200 generated and used to transform *Arabidopsis* wild type leaf protoplasts. When GFP alone is
201 expressed, green fluorescent signals were mainly detected in the cytosol (Fig. 4B). On the
202 other hand, protoplasts expressing SVR9-GFP or SVR9L1-GFP showed signals that clearly
203 aligned with chlorophyll autofluorescence, confirming the chloroplast localization of both
204 proteins (Fig. 4B). Taken together, our results demonstrate that SVR9 and SVR9L1 encode the
205 chloroplast translation initiation factor IF3 proteins.

206 Lastly, we examined the tissue expression pattern of SVR9. A ~1.9 kb promoter region
207 upstream of SVR9 start codon was transcriptionally fused with the *GUS* gene and introduced
208 into wild type *Arabidopsis*. Histochemical GUS staining was performed in *P*_{SVR9}:*GUS* lines at
209 various developmental stages. In general, strong GUS activities were detected in
210 photosynthetic tissues while GUS levels were below the detection limit in roots (Fig. 4C). In
211 addition, SVR9 showed stronger expressions in young, newly emerged leaves as compared to
212 the gradually reducing expressions in older leaves (Fig. 4C and 4D). These observations
213 suggest that the expression of SVR9 is regulated by leaf developmental stages and the need

214 for SVR9 activities is probably higher in actively growing young tissues, consistent with the
215 virescent mutant phenotypes.

216

217 **Genetic interactions between *svr9-2*, *svr9II-1* and *var2***

218 To further dissect the functions of *SVR9* and *SVR9LI*, and their interactions with *var2*,
219 we sought for additional mutant alleles of these two genes. For *SVR9*, we obtained a SAIL T-
220 DNA insertion line SAIL_172_F02 and confirmed that the T-DNA was located in the last
221 exon of *SVR9*, 175 bp upstream of the stop codon, and this allele was named *svr9-2*
222 (Supplemental Fig. S4). For *SVR9LI*, we obtained a SALK T-DNA insertion line
223 SALK_140431C, which harbored a T-DNA in the 6th intron, and this mutant allele was
224 named *svr9II-1* (Supplemental Fig. S4). In contrast to the virescent phenotype of *svr9-1*,
225 *svr9-2* showed an overall wild type-like phenotype and reduced accumulation of *SVR9*
226 transcripts, suggesting that it is a weaker allele of *SVR9* (Supplemental Fig. S4). Similarly,
227 *svr9II-1* mutants were also indistinguishable from wild type (Supplemental Fig. S4). Double
228 mutants of *svr9-2* and *svr9II-1* also resembled wild type (Supplemental Fig. S4).

229 We next examined the genetic interactions between *svr9-2*, *svr9II-1* and two *var2* mutant
230 alleles, *var2-4* and *var2-5* (Supplemental Fig. S5). To evaluate the extent of leaf variegation
231 in a quantitative manner, images of the first true leaves from each genotype were converted to
232 greyscale and distributions of the pixel intensity values of these images were generated and
233 compared. Green sectors of a leaf will have a lower pixel intensity value while white sectors
234 contain pixels with higher intensity values. Uniform leaf color will give rise to a distribution
235 with a relatively narrow peak. In contrast, variegated leaf images have broader peaks and
236 contain more pixels of higher intensity values. Analysis of wild type, *var2-5* and *var2-4* leaf
237 images showed that they each display a distinctive pattern of pixel intensity histogram that
238 correlates well with the degree of variegation (Fig. 5A and 5E). On the other hand, *svr9II-1*,
239 *svr9-2* and *svr9II-1 svr9-2* leaves are not only visually indistinguishable from wild type but
240 also have pixel intensity histograms similar to that of wild type (Fig. 5B and 5F). Double
241 mutants of *svr9II-1* with *var2-5* or *var2-4* showed leaf variegation that resembled *var2-5* and
242 *var2-4*, respectively, suggesting that *svr9II-1* alone does not significantly alter *var2* leaf
243 variegation (Fig. 5C and 5D). In contrast, double mutants of *svr9-2* with *var2-5* or *var2-4*
244 showed reduced leaf variegation than *var2-5* and *var2-4*, respectively, suggesting that a
245 weaker allele of *SVR9* can partially suppress *var2* leaf variegation (Fig. 5C and 5D). The
246 stronger effects of *svr9-2* compared to *svr9II-1* in suppressing *var2* variegation were also
247 clearly reflected by the shifts observed in the histograms of *svr9-2 var2* and *svr9II-1 var2*
248 double mutant leaf images (Fig. 5G and 5H). Interestingly, leaf variegation was almost absent
249 in *svr9II-1 svr9-2 var2* triple mutants (Fig. 5C-5D, 5G-5H). The fact that *var2* leaf
250 variegation was suppressed to a stronger degree in the *svr9II-1 svr9-2* background than in the

251 *svr9-2* mutant alone suggested an additive effect of *svr9II-1* and *svr9-2* on suppressing *var2*
252 leaf variegation. Together, these data suggest that despite their overall wild type appearances,
253 *svr9II-1*, *svr9-2*, and *svr9II-1 svr9-2* mutants possess molecular phenotypes, and these
254 phenotypes can modify *var2* leaf variegation.

255

256 **Chloroplast translation initiation factor IF3 activities are essential for plant** 257 **development**

258 Given the high homology between *SVR9* and *SVR9LI*, we next tested the functional
259 relationship between these two genes. As *svr9-2 svr9II-1* double mutants resembled wild
260 type, we sought to obtain *svr9-1 svr9II-1* double mutants. However, extensive genotyping did
261 not identify double mutants homozygous for both *svr9-1* and *svr9II-1*. We did recover mutant
262 plants that were homozygous for *svr9-1* but heterozygous for *svr9II-1* (referred to as *svr9-1*
263 *svr9II-1/+* hereafter), which showed a stronger virescent phenotype and smaller stature than
264 *svr9-1* alone (Fig. 6A). Genotyping the selfed progeny of *svr9-1 svr9II-1/+* did not yield the
265 expected double mutants either. In the siliques of *svr9-1 svr9II-1/+* plants, we observed an
266 increased occurrence of abortive seeds (Fig. 6B). In addition, we generated transgenic plants
267 in *svr9-1* background that expressed *SVR9LI* under the control of the 35S promoter. The over-
268 expression of *SVR9LI* effectively rescued the virescent phenotype of *svr9-1* (Fig. 6C). These
269 data suggest that: 1) *SVR9* and *SVR9LI* are functionally redundant; 2) *svr9-1 svr9II-1* is likely
270 lethal and 3) chloroplast IF3 activities are essential for chloroplast and plant development.

271

272 **Compromised chloroplast translation initiation factor IF3 activities lead to leaf** 273 **developmental defects**

274 During the investigation of mutant alleles of *SVR9* and *SVR9LI* and their genetic
275 interactions, we noticed a number of leaf developmental defects in *svr9-1* and *svr9-1 svr9II-1/+*.
276 First, leaf margin development was perturbed in these mutants. *svr9-1* displayed a more
277 serrated leaf margin compared to that of wild type (Fig. 7A). Leaf margins of *svr9II-1*
278 resembled wild type, consistent with its wild type appearance (Fig. 7A). However, *svr9-1*
279 *svr9II-1/+* plants showed an even more pronounced leaf margin serration compared to either
280 of the single mutant (Fig. 7A). The increased leaf serrations from *svr9-1* to *svr9-1 svr9II-1/+*
281 was further validated by the quantitative analysis of leaf shape based on three different
282 parameters, the leaf dissection index ($\text{perimeter}^2/4\pi \times \text{leaf area}$), the number of teeth/leaf
283 perimeter, and the tooth area/leaf area (Royer et al., 2008; Bilsborough et al., 2011) (Fig. 7B-
284 7D). These analyses suggest that decreased activities of chloroplast IF3s promotes the
285 initiation and the outgrowth of leaf lobes. However, we did not observe major leaf serration
286 changes in *svr8-2*, a null mutant lacking the chloroplast ribosomal protein L24, suggesting

287 that not all mutants of chloroplast translation display abnormal leaf margin development
288 (Supplemental Fig. S6; Liu et al., 2013).

289 Second, we examined the leaf anatomy of these mutants. Cross sections of wild type
290 leaves reveal the organized arrangement of palisade and spongy mesophyll (Fig. 7E). In *svr9-*
291 *1*, palisade mesophyll can still be distinguished but is less organized than that of wild type
292 (Fig. 7E). Leaf mesophyll was more dramatically affected in *svr9-1 svr9II-1/+*, in which the
293 distinction between palisade and spongy mesophyll became obscure and intercellular air
294 space appeared to be increased (Fig. 7E).

295 Third, we discovered that leaf vascular development is also altered in *svr9-1* and *svr9-1*
296 *svr9II-1/+* mutants, as indicated by the cotyledon venation patterns. We used the number of
297 closed areoles in mature cotyledons as an indicator of leaf vascular development (Sieburth,
298 1999). In wild type, cotyledons with two, three and four areoles were common. In *svr9-1*,
299 although the predominant portions of cotyledons show two or three areoles, cotyledons with
300 only one areole were identified in *svr9-1* (Table 1; Fig. 7F). The defects were more
301 conspicuous in *svr9-1 svr9II-1/+*. The percentage of three or four areoles were drastically
302 decreased in *svr9-1 svr9II-1/+* (Table 1; Fig. 7F). Moreover, cotyledons with no closed
303 areoles can be identified in *svr9-1 svr9II-1/+* (Table 1; Fig. 7F). Abnormal leaf vascular
304 development is not generally associated with defects of chloroplast development as we did
305 not observe major cotyledon venation changes in an albino mutant *svr4-2* we reported earlier
306 (Supplemental Table S1; Yu et al., 2011).

307 Taken together, our data show that the down-regulated chloroplast translation initiation
308 factor IF3 activities alter leaf margin, mesophyll and vascular development.

309

310 **Chloroplast translation defects alter auxin homeostasis**

311 Phytohormone auxin has been implicated in the regulation of leaf margin and vascular
312 development (Scarpella et al., 2006; Bilsborough et al., 2011). Given the margin and vascular
313 defects of *svr9-1* and *svr9-1 svr9II-1/+*, we explored whether auxin homeostasis was altered
314 in the mutants. To monitor auxin homeostasis, we crossed an auxin reporter line *DR5:GUS*
315 into *svr9-1* and *svr9-1 svr9II-1/+* mutant backgrounds, respectively. GUS staining of
316 *DR5:GUS* reporter line seedlings revealed auxin maxima at cotyledon tips, consistent with
317 previous reports (Ulmasov et al., 1997). In contrast, stronger and more expanded *DR5:GUS*
318 signals were observed in *svr9-1* background compared to that of the *DR5:GUS* reference
319 plants (Fig. 8A and 8B). Clear signals can be observed along the leaf margin in *svr9-1*
320 *DR5:GUS* plants (Fig. 8B). A stronger increase in the *DR5:GUS* staining was observed in the
321 *svr9-1 svr9II-1/+* background (Fig. 8C). If the mutations of chloroplast IF3s can lead to
322 abnormal auxin homeostasis, one would expect that the inhibition of chloroplast translation
323 might also cause similar alterations in auxin homeostasis. To test this hypothesis, we treated

324 *DR5:GUS* reporter plants with chemical inhibitors of prokaryotic translation,
325 chloramphenicol and spectinomycin, respectively. Compared to plants subjected to the mock
326 treatments, both chloramphenicol and spectinomycin treatments led to stronger and more
327 diffused distributions of auxin signals (Fig. 8D-8F). These data suggest that disturbances in
328 chloroplast translation induced by mutations or pharmacological treatments can affect auxin
329 homeostasis.

330 We next tested whether auxin homeostasis can impact the development of leaf margins of
331 *svr9-1* and *svr9-1 svr9II-1/+*. Mutant plants were treated with auxin transport inhibitor 2,3,5-
332 triiodobenzoic acid (TIBA) or *N*-1-naphthylphthalamic acid (NPA). Compared with mock
333 treatments, *svr9-1* and *svr9-1 svr9II-1/+* lost the serrated leaf margins upon TIBA or NPA
334 treatments (Fig. 9A and 9B). Consistent with the visual observations, statistical analysis
335 showed that both TIBA and NPA treatments greatly reduced the leaf dissection index of *svr9-1*
336 *1* and *svr9-1 svr9II-1/+* (Fig. 9C and 9D). These results indicate that artificially altering auxin
337 homeostasis by drugs could modulate *svr9-1* and *svr9-1 svr9II-1/+* mutant leaf margins.
338

339 ***CUC2* is involved in the regulation of leaf margin development mediated by chloroplast** 340 **translation initiation factor IF3s**

341 It is well established that NAC family transcription factor CUP-SHAPED
342 COTYLEDON2 (*CUC2*) is a central regulator in auxin-mediated leaf margin development
343 (Nikovics et al., 2006; Kawamura et al., 2010; Bilsborough et al., 2011). To dissect
344 genetically the regulation of leaf margin by chloroplast IF3s, we investigated the genetic
345 interactions between *SVR9*, *SVR9LI* and *CUC2*. We obtained a *CUC2* loss-of-function mutant
346 SALK_035713 (named *cuc2-101* hereafter) and a gain-of-function mutant *cuc2-1D* (Larue et
347 al., 2009). Consistent with previous reports, *cuc2-101* showed a smooth leaf margin while
348 *cuc2-1D* displayed a more serrated leaf margin (Fig. 10A; Nikovics et al., 2006; Larue et al.,
349 2009). We next crossed *svr9-1* and *svr9-1 svr9II-1/+* into the *cuc2-101* and *cuc2-1D*
350 background, respectively. Overall, the presence of *cuc2-101* mutation greatly suppressed the
351 leaf dissection index, the number of teeth/leaf perimeter, and the tooth area/leaf area in *svr9-1*
352 (Fig. 10A-10D). Similar suppression of leaf serrations by *cuc2-101* was also observed in
353 *svr9-1 svr9II-1/+*, albeit to a less extent (Fig. 10A-10D). On the other hand, the addition of
354 *cuc2-1D* to *svr9-1* increased leaf serration based on the three parameters we monitored (Fig.
355 10B-10D). In *svr9-1 svr9II-1/+* background, introduction of *cuc2-1D* mutation has no
356 obvious impact on the leaf dissection index and the number of teeth/leaf perimeter, but *cuc2-1D*
357 *1D* did increase the tooth area/leaf area in *svr9-1 svr9II-1/+* (Fig. 10B-10D). This is
358 consistent with previous notion that increased *CUC2* expression promotes leaf marginal
359 serrations mostly by increasing the lobe outgrowth (Kawamura et al., 2010). Our observations
360 suggest that *svr9-1* and *svr9-1 svr9II-1/+*-mediated leaf margin development involves *CUC2*.

361 Interestingly, despite the genetic interaction between *CUC2* and *SVR9/SVR9L1* on the
362 leaf shape characteristics, neither *cuc2* mutants affects the virescent leaf color phenotype of
363 *svr9-1* or *svr9-1 svr9L1-1/+* (Fig. 10A; Supplemental Fig. S7). Together the genetic
364 interactions between *SVR9* and *CUC2* suggest that *SVR9* and *SVR9L1*-mediated leaf margin
365 development is dependent on *CUC2* activities and is independent of their roles in chloroplast
366 development.

367

368 Discussion

369 Chloroplast translation initiation factor IF3 activities are essential for chloroplast and 370 plant development

371 We are interested in using *var2* as a tool to gain insight into the genetic regulation of
372 chloroplast development (Liu et al., 2010a). In this study, we isolated a new *var2* genetic
373 suppressor locus termed *SUPPRESSOR OF VARIEGATION9* (*SVR9*). We showed that *SVR9*
374 encodes a chloroplast protein bearing high homology to prokaryotic translation initiation
375 factor IF3. In addition, *svr9-1* mutant phenotypes were fully complemented by a bacterial IF3
376 directed by the chloroplast transit peptide of *SVR9*. Taken together, we showed conclusively
377 that *SVR9* codes for a *bona fide* chloroplast translation initiation factor IF3.

378 In *Arabidopsis thaliana*, there are three genes that are annotated to code for prokaryotic
379 type translation initiation factor IF3 (Nesbit et al., 2015). Besides *SVR9*, we showed that a
380 close homologue of *SVR9*, which we named *SVR9-LIKE1* (*SVR9L1*), is also a chloroplast
381 protein, while the third gene product is a mitochondrial protein (Nesbit et al., 2015). This
382 complement of prokaryotic type IF3s is consistent with the endosymbiotic origins of the two
383 organelles. For chloroplast-localized *SVR9* and *SVR9L1*, multiple pieces of evidence suggest
384 that they share redundant functions in chloroplast development. *SVR9* and *SVR9L1* share the
385 same gene structures and high homology at amino acid sequence level (Fig. 4A,
386 Supplemental Fig. S1), suggesting that they may have evolved through gene duplication.
387 Functionally, *svr9-1* can be fully rescued by the over-expression of *SVR9L1* (Fig. 6C).
388 Moreover, genetic interaction studies revealed that the combined activities of *SVR9* and
389 *SVR9L1* are essential for chloroplast and plant development, as we were not able to recover
390 double homozygous mutants for *svr9-1* and *svr9L1-1*. Based on the severity of *svr9-1* and
391 *svr9L1-1* mutant phenotypes, it is likely that *SVR9* contributes more to the overall chloroplast
392 IF3 activities while *SVR9L1* plays a relatively minor role, and the genetic relationship
393 between *SVR9* and *SVR9L1* indicates an unequal functional redundancy (Briggs et al., 2006).

394 Three prokaryotic translation initiation factors, IF1, IF2 and IF3, are employed by the
395 70S ribosome, and IF3 has been proposed to be responsible for sensing translation initiation
396 regions of mRNAs and ensuring initiation fidelity (Lomakin et al., 2006; Milon et al., 2008).
397 Our results indicate that chloroplast translation initiation factor IF3 activities, contributed by

398 both SVR9 and SVR9L1 in *Arabidopsis* chloroplasts, are indispensable for chloroplast and
399 plant development. Previous studies have indicated that chloroplast translation initiation
400 factor IF2 activities are also essential for plant development (Miura et al., 2007). These data
401 suggest that the proper initiation of translation in the chloroplast is essential for chloroplast
402 biogenesis.

403

404 **The suppression of *var2* leaf variegation by *SVR9* and *SVR9L1* mutations**

405 Previously we have proposed a threshold model to explain the mechanisms of leaf
406 variegation mediated by VAR2/AtFtsH2 (Yu et al., 2004; 2005). The core of our model is that
407 the development of functional chloroplasts requires a threshold level of thylakoid FtsH
408 complexes/activities. Moreover, we envisioned that this threshold would be dynamic, and
409 changing functional or developmental status of the chloroplast may necessitate different
410 thresholds. Based on the model, we should be able to identify functional or developmental
411 processes that, when disrupted, may modify the threshold and the need for FtsH activities. To
412 this end, we carried out *var2* genetic suppressor screens. In these genetic suppressors of *var2*,
413 we propose that the suppressor mutations lead to disturbed functional or developmental
414 chloroplast states that lowers the endogenous threshold for VAR2/AtFtsH2. Through both our
415 work with the *SUPPRESSOR OF VARIATION* loci and work from other groups, a
416 definitive link between the threshold and some aspects of chloroplast translation has been
417 established (Miura et al., 2007; Yu et al., 2008; Liu et al., 2010b; 2010c; 2013). However, a
418 key aspect of the threshold model, i.e. a multi-point correlation of the changing functional or
419 developmental states of the chloroplast with the corresponding changing needs for FtsH
420 activities, remained hypothetical. In this study, through multiple mutant alleles and mutant
421 combinations of *SVR9* and *SVR9L1*, we were able to create a series of chloroplast
422 developmental states and explore this important aspect of the threshold hypothesis. In wild
423 type background where chloroplast IF3s are at full capacity, VAR2/AtFtsH2 activities are
424 necessary for chloroplast development and the lack of VAR2/AtFtsH2 causes leaf variegation.
425 The *svr9L1-1* mutation slightly reduces IF3 activities, but functional VAR2/AtFtsH2 is still
426 required and leaf variegation is not suppressed. However, in *svr9-2*, the reduction of IF3
427 activities is greater than in *svr9L1-1*. The state generated by *svr9-2* may lower the threshold
428 need for VAR2/AtFtsH2 and leaf variegation reduces. IF3 activities are further reduced in
429 *svr9L1-1 svr9-2* double mutants, and the mutant background of *svr9L1-1 svr9-2* generated a
430 state that the need for VAR2/AtFtsH2 activities is no longer necessary for chloroplast
431 development, thus a full suppression of leaf variegation. When IF3 activities is further
432 reduced in *svr9-1* and *svr9-1 svr9L1-1/+* mutants, the lack of IF3 activities itself starts to
433 impair chloroplast development and mutant plants display a clear visual phenotype, and this

434 functional state bypass the need for VAR2/AtFtsH2, as observed in our previous *var2*
435 suppressor mutants (Liu et al., 2010a; Putarjunan et al., 2013).

436 Several messages can be gathered from these data. First, our genetic data indicate that
437 full wild type level of IF3 activities are not necessary for chloroplast development under lab
438 conditions, as *svr9II-1*, *svr9-2*, and *svr9II-1 svr9-2* resembled wild type. However, a key
439 message from our data is that a superficial wild type appearance does not necessarily mean a
440 lack of phenotypes at molecular level. In this sense, genetic suppressor screens can be a very
441 sensitive and powerful approach to uncover subtle molecular alterations in mutants. Second,
442 the different mutants and mutant combinations in our study generated different chloroplast
443 states where VAR2/AtFtsH2 functions may be partially or completely bypassed, supporting
444 our previous hypothesis that the threshold for FtsH activities can vary.

445

446 **The interaction between chloroplast and leaf development**

447 The chloroplast is the site for photosynthesis, as well as the venue for the synthesis of
448 numerous metabolic and regulatory molecules such as phytohormones, and the proper
449 functioning of the chloroplast is essential for plant growth and development. It is thus not
450 surprising that the functional or developmental states of the chloroplast can impact processes
451 outside of the chloroplast. Previous studies have established multiple regulatory pathways that
452 coordinate the states of the chloroplast with gene expressions in the nucleus. In addition, it is
453 widely known that plant leaf development is also linked with the states of the chloroplast.
454 However, we lack detailed information regarding the relationship between leaf development
455 and the chloroplast.

456 In this study, we uncovered a range of leaf developmental phenotypes in *SVR9* and
457 *SVR9L1* mutants that may be linked with altered auxin homeostasis and auxin regulated
458 pathways. First, we discovered that the cotyledon venation patterns were abnormal in *svr9-1*
459 and *svr9-1 svr9II-1/+* mutants. Overall, we observed that mutant cotyledons showed a trend
460 of reduced complexity of vascular development as indicated by the numbers of areoles (Fig.
461 7F; Table 1). It is generally believed that auxin is a central regulator of leaf vascular
462 development, thus the venation pattern changes in the mutants may reflect an altered auxin
463 homeostasis (Sieburth, 1999; Cheng et al., 2007). Second, we observed that leaf margins are
464 more serrated in *svr9-1* and *svr9-1 svr9II-1/+* mutants than those of the wild type (Fig. 7A-
465 7D). The induction of leaf serrations are dictated by a feedback loop of auxin maxima
466 established by PIN1 convergence points and CUC2 activities (Bilsborough et al., 2011). The
467 expression of CUC2 promotes the formation of PIN1 convergence points and in turn the
468 auxin maxima along the leaf margin where CUC2 expressions are then repressed by auxin
469 (Bilsborough et al., 2011). This feedback regulation of CUC2, PIN1 and auxin level
470 eventually leads to the alternate presence of CUC2 expressions at leaf indentations and auxin

471 maxima at leaf protrusions (Bilsborough et al., 2011; Byrne, 2012). Thirdly, we observed
472 alterations in auxin homeostasis in *svr9-1* and *svr9-1 svr9L1-1/+* mutants as indicated by the
473 changes in *DR5:GUS* expression patterns (Fig. 8A-8C). Changes in auxin homeostasis can
474 also be observed in plants treated with chloroplast translation inhibitors (Fig. 8D-8F).
475 Treatments with auxin transport inhibitors can alter the leaf margin phenotypes of *svr9-1* and
476 *svr9-1 svr9L1-1/+* mutants (Fig. 9). These data suggest that auxin may play an important role
477 in leaf developmental processes regulated by chloroplast IF3s. Surprisingly, we did not
478 observe altered leaf margins in *svr8-2*, a null mutant of the chloroplast ribosomal protein L24
479 (Supplemental Fig. S6; Liu et al., 2013). It is possible that when individual components of the
480 chloroplast translation system were mutated, chloroplast translation is affected in such a
481 manner that may or may not trigger the abnormal development of leaf margins. This raises the
482 interesting possibility that specific aspects of chloroplast translation are associated with leaf
483 margin development. Last but not least, our genetic data support the notion that chloroplast
484 IF3s SVR9 and SVR9L1 regulate leaf margin development at least partially via the *CUC2*-
485 mediated pathway since a lack of *CUC2* greatly hampered but not completely abolished the
486 manifestation of leaf margin phenotypes of *svr9-1* and *svr9-1 svr9L1-1/+* (Fig. 10). The
487 genetic interaction results further suggest that there may be other factors involved in the
488 output of the retrograde signals from the *svr9-1 svr9L1-1/+* mutant chloroplasts (Fig. 10).
489 Based on our data, it is clear that certain functional states of the chloroplast, as generated by
490 the lack of *SVR9* and *SVR9L1*, are able to regulate leaf development. It is possible that these
491 states of the chloroplast are capable of altering the auxin homeostasis, which in turn regulates
492 *CUC2* activities. It is also possible that these states influence auxin and *CUC2* separately.
493 Although the precise mechanisms remain to be elucidated, it is tempting to speculate that
494 these functional states may generate retrograde signals that coordinate the states of the
495 chloroplast with leaf development.

496

497 **Conclusions**

498 Taken together, our data indicate that chloroplast translation initiation factor IF3
499 activities are essential for plant and chloroplast development. Mutations in the chloroplast
500 translation initiation factor IF3s can suppress the leaf variegation phenotype of *var2* mutants.
501 Moreover, our data indicate that the functional or developmental states of the chloroplast can
502 regulate leaf development, particularly the processes that are associated with auxin. Currently
503 we do not know whether this regulation involves the known retrograde signaling pathways or
504 it represents a new route of signaling, and future research will undoubtedly expand our
505 understanding of the intricate relationship between the chloroplast and the rest of the plant
506 cell.

507

508 **Materials and methods**

509 **Plant materials and growth conditions**

510 All *Arabidopsis thaliana* strains used in this study are of the Columbia-0 background.
511 *svr9-1* was isolated in this study. The T-DNA insertion lines SAIL_172_F02 (*svr9-2*),
512 SALK_140431C (*svr911-1*), SALK_035713 (*cuc2-101*) and *cuc2-ID* were obtained from the
513 Arabidopsis Biological Resource Center (ABRC); *svr4-2* and *svr8-2* have been described (Yu
514 et al., 2011; Liu et al., 2013). Seeds were sown on commercial soil mix (Pindstrup, Denmark)
515 or on half strength Murashige and Skoog (1/2 MS) medium supplemented with 1% sucrose,
516 and stratified for two days at 4°C before placed in growth rooms. When solid medium was
517 needed, 0.8% agar (w/v) was added to the 1/2 MS medium. *Arabidopsis* plants were
518 maintained at ~22 °C under continuous illumination (~100 $\mu\text{mol m}^{-2} \text{s}^{-1}$).

519

520 **Chlorophyll content measurements**

521 Fresh plant tissues were harvested, weighed, and finely ground in liquid N₂. Total
522 chlorophyll was extracted with 95% ethanol. Chlorophyll contents were determined as
523 described (Lichtenthaler, 1987). Chlorophyll measurements of different samples were
524 normalized on a fresh tissue weight basis. Each sample consisted of leaf tissues pooled from 2
525 to 4 individual plants. Mean chlorophyll content of leaf tissues of each genotype was
526 calculated from three independent pooled leaf samples. Differences in chlorophyll content
527 between WT and mutants were evaluated with *p* values generated by *t*-test.

528

529 **Map-based cloning**

530 The *SVR9* locus was initially mapped by the bulked segregation analysis using a pool of
531 95 F₂ mutant seedlings from a cross between *svr9-1* and Landsberg *erecta* (Lukowitz et al.,
532 2000). A mapping population consisting of 570 F₂ mutant plants was used to further fine map
533 the *svr9-1* mutation. Primers of the molecular markers generated in this study were listed in
534 Supplemental Table S2. Primers used to amplify various At2g24060 genomic fragments were
535 listed in Supplemental Table S2.

536

537 **Semi-quantitative RT-PCR analysis**

538 Total cellular RNAs were purified using Trizol RNA reagent (Life Technologies, CA,
539 USA) following the manufacturer's instructions and stored at -80 °C. For semi-quantitative
540 RT-PCR analysis, first strand cDNAs were synthesized from 1 μg DNase I treated total RNAs
541 using a PrimeScript reverse transcription kit (Takara, Japan). The gene-specific primers were
542 listed in Supplementary Table S2.

543

544 **Functional Complementation of *svr9-1***

545 All primers used in vector construction were listed in Supplementary Table S2. To
546 complement *svr9-1*, full-length cDNAs of *SVR9/At2g24060* and *SVR9L1/At4g30690* were
547 amplified using primers 24060F and 24060R, and 30690F and 30690R, respectively. The
548 amplified fragments were cloned into pBluescript KS+ (pBS) and sequenced before
549 subcloned into a binary vector pBII11L (Yu et al., 2004). The resulting constructs were
550 named *P_{35S}:At2g24060* and *P_{35S}:At4g30690*, respectively.

551 To express *E. coli* IF3 infC in *Arabidopsis*, the coding sequence of *infC* was amplified
552 from *E. coli* genomic DNA using primers *E. coli* IF3-F and *E. coli* IF3-R and cloned into
553 pBS. The coding sequence of the chloroplast transit peptide (cTP) region of SVR9 (1-71 aa of
554 SVR9) was amplified with cTPF and cTPR and cloned into pBS. After sequencing pBS-infC
555 and pBS-SVR9cTP, the *infC* and *SVR9cTP* were sequentially subcloned into pBII11L to have
556 SVR9cTP fused in frame at N-terminal of infC. The resulting construct was named
557 *P_{35S}:cTP_{SVR9}-infC*.

558 Each of the binary vectors was transformed into *Agrobacterium tumefaciens* by
559 electroporation, and the floral dip method was used for *Arabidopsis* transformation (Clough
560 and Bent, 1998). T1 transgenic lines were screened on solid 1/2 MS medium containing 50
561 mg·L⁻¹ kanamycin.

562

563 **Protoplast transient expression assays**

564 To transiently express C-terminal GFP fusion proteins SVR9cTP-GFP, SVR9-GFP and
565 SVR9L1-GFP in leaf protoplasts, the coding sequences of SVR9cTP, SVR9 and SVR9L1
566 were cloned into pTF486 to fuse in frame with GFP coding sequences (Yu et al., 2008). Fresh
567 prepared wild type *Arabidopsis* mesophyll protoplasts were transformed with each of the
568 transient expression vectors following the procedures described in Yoo et al. (2007). After
569 transformation, protoplasts were incubated overnight and examined with confocal microscopy
570 using the Apo TIRF 60x Oil objective (N.A. 1.49) (Nikon A1). GFP and chlorophyll
571 autofluorescence signals were monitored through 525/50 and 700/75 emission filters,
572 respectively.

573

574 **Histochemical GUS staining**

575 To generate *SVR9* promoter-β-glucuronidase (GUS) transcriptional fusion construct, a
576 1913 bp genomic DNA fragment upstream of the start codon of *SVR9* gene was amplified
577 using primers 24060PF-XbaI2 and 24060PR-BamHI2 and cloned into pCB308 (Xiang *et*
578 *al.*,1999). The resulting construct was used to transform wild type *Arabidopsis* plant.
579 *P_{SVR9}:GUS* lines were screened based on Basta resistance. GUS activities were assayed in T1
580 and T2 generations (Jefferson, 1987).

581 To test the impact of *svr9-1* and *svr9II-1* mutations on *DR:GUS* expression patterns,
582 *DR5:GUS* reporter gene was introduced to *svr9-1* and *svr9-1svr9II-1/+* via genetic crossing.
583 *DR5:GUS* activities in different genetic backgrounds were assayed in 6-day-old seedlings.
584

585 **Quantification of leaf variegation**

586 The first true leaves of two-week-old *Arabidopsis* seedlings were hand cut and mounted
587 in water. Images of each individual leaf were captured using a stereoscope (Nikon, SMZ25)
588 equipped with a CCD camera (Nikon, DS-U3). All leaves were photographed with the same
589 settings. To quantify the extent of variegation, leaf images were first converted to grayscale
590 using the ImageJ software. Pixels constituting the leaf blade were selected and intensity values
591 of these pixels were obtained using the NIS-Elements software (Nikon). Frequency was
592 calculated as number of pixels of each intensity value (ranging from 0-255)/number of pixels
593 constituting the leaf blade area. Frequency distributions of pixel intensity values of each leaf
594 image were generated using the GraphPad Prism software. The quantification of leaf
595 variegation was repeated three times. Similar patterns of frequency distributions of pixel
596 intensity values were obtained for each repeat.
597

598 **Leaf margin analysis**

599 Water mounted individual leaves were photographed using a stereoscope (Nikon,
600 SMZ25) equipped with a CCD camera (Nikon, DS-U3). Three parameters that were
601 commonly used in leaf margin analysis including: the leaf dissection index
602 ($\text{perimeter}^2/4\pi \times \text{leaf area}$), the number of teeth/leaf perimeter, and the tooth area/leaf area,
603 were used in this study to quantify the differences in leaf margin (Royer et al., 2008;
604 Bilsborough et al., 2011). Leaf blade region (excluding leaf petiole) was used in quantitative
605 analyses. Leaf area and perimeter measurements were performed using the ImageJ software.
606 Graphs were generated by the GraphPad Prism software. Differences between means of each
607 leaf shape parameter were evaluated by *p* values generated by *t*-test.
608

609 **Analysis of leaf cross sections and cotyledon vein patterns**

610 Basal parts of the first of true leaf of 10-day-old wild type, *svr9-1* and *svr9-1 svr9II-1/+*
611 were hand cut and infiltrated with fixation solution (4% (v/v) glutaraldehyde in 0.1 mM
612 sodium phosphate buffer, pH6.8). Fixed tissues were dehydrated and embedded in Technovit
613 7100 resin (EMS, PA, USA). Semi-thin sections (10 μm) prepared with a microtome
614 (RM2265, Leica) were stained with 1% (v/v) toluidine blue O and observed with a Leica
615 DM5000B microscope equipped with a DFC425C CCD camera.

616 To observe cotyledon veins, cotyledons of 10-day-old plants were hand cut and
617 decolored in 70% ethanol until the veins became clearly visible. Decolored cotyledons were

618 then photographed with a digital camera mounted on a stereo microscope. Cotyledon vein
619 patterns were categorized based on the number of areoles formed (Sieburth, 1999)

620

621 **Chemical treatments**

622 All chemicals used in this study were purchased from Sigma unless otherwise specified.
623 1-N-naphthylphthalamic acid (NPA) and 2,3,5-Triiodobenzoic acid (TIBA) were dissolved in
624 dimethyl sulfoxide (DMSO). Wild type, *svr9-1* and *svr9-1 svr9II-1/+* seeds were germinated
625 and grown on solid 1/2 MS medium supplemented with 1 μ M NPA or 1 μ M TIBA. Plants
626 grown on solid 1/2 MS medium with equal concentration of DMSO served as controls.
627 Images of the third true leaves in 2-week-old plants were examined.

628 To test *DR5:GUS* expression in response to chloroplast translation inhibitors, *DR5:GUS*
629 lines of different genetic backgrounds were germinated and grown on liquid 1/2 MS medium
630 for 6 days before adding chloramphenicol or spectinomycin to a final concentration of 5 mM.
631 Equal amounts of ethanol were added as the mock treatment. After 24 hours of treatment,
632 seedlings were harvested and assayed for GUS activities. Plant liquid cultures were shaken at
633 120 rpm to keep the seedlings floating.

634

635 **Accession numbers**

636 Sequence data from this article can be found in the The *Arabidopsis* Information Resource
637 (TAIR) or GenBank/EMBL databases under the following accession numbers: SVR9,
638 At2g24060; SVR9L1, At4g30690; VAR2/AtFtsH2, At2g30950; CUC2, At5g53950, *E. coli*
639 infC, NP_416233.1.

640

641 **Supplemental data**

642 **Supplemental Table S1.** Comparison of cotyledon vein patterns of wild type and *svr4-2*.

643 **Supplemental Table S2.** Primers used in this study.

644 **Supplemental Figure S1.** Protein sequence alignments of SVR9/At2g24060,

645 SVR9L1/At4g30690, At1g34360 and *E. coli* infC.

646 **Supplemental Figure S2.** Chloroplast localization of cTP_{SVR9}-GFP.

647 **Supplemental Figure S3.** Phylogenetic analysis of prokaryotic IF3-like proteins from *E. coli*
648 and representative photosynthetic species.

649 **Supplemental Figure S4.** Identification of *svr9-2* and *svr9II-1*.

650 **Supplemental Figure S5.** Whole plant phenotypes of representative 2-week-old plants of the
651 same genotypes shown in Fig. 5A-5D.

652 **Supplemental Figure S6.** Comparison of leaf margin development in WT, *svr9-1* and *svr8-2*.

653 **Supplemental Figure S7.** Whole plant phenotypes of representative 2-week-old plants of the
654 same genotypes shown in Fig. 10A.

655 **Figure legends**

656 **Figure 1.** Suppression of *var2* leaf variegation by *svr9-1*. A, Representative 15-day-old wild
657 type (WT), *var2-5, 092-004 (var2-5 svr9-1)*, and *svr9-1* plants. C, Representative 15-day-old
658 WT, *var2-4, svr9-1*, and *var2-4 svr9-1* double mutant. B and D, Chlorophyll contents of
659 indicated tissues in plants shown in A and C, respectively. Total: entire rosettes excluding the
660 cotyledons; Peripheral: the first two true leaves; Center: rosettes excluding the cotyledons and
661 the first two true leaves. Chlorophyll measurements were normalized on a fresh tissue weight
662 basis. Data were presented as mean \pm standard deviation (s.d.) of three biological replicates.
663 *: $0.01 < p < 0.05$; **: $p < 0.01$.

664

665 **Figure 2.** Cloning of *SVR9*. A, Schematic representation of the positional cloning procedure
666 used to identify *svr9-1* mutation. Primers of the molecular markers designed in this study
667 were listed in Supplemental Table S2. A total of 570 F2 plants (1140 chromosomes) were
668 used in fine mapping. Numbers of recombinants were marked under each molecular marker.
669 The asterisk indicated the position of *SVR9* (At2g24060). In the gene model, boxes represent
670 exons and lines represent introns. 5' and 3' untranslated regions (UTRs) were shaded. Arrows
671 represent the positions of the primers used in B and C. B, PCR analyses using various primer
672 combinations indicated that At2g24060 genomic regions were disrupted in *svr9-1*. C, Semi-
673 quantitative RT-PCR analyses of the accumulations of *SVR9* transcripts in wild type and *svr9-1*
674 *1* using indicated primer combinations. Expression of *ACT2* was used as an internal control.

675

676 **Figure 3.** Complementation of *svr9-1* and *092-004*. A, Leaf color phenotypes of two-week-
677 old WT, *svr9-1*, *var2-5, 092-004* and representative lines overexpressing At2g24060 in *svr9-1*
678 or *092-004* background. B, Leaf color phenotypes of two-week-old WT, *svr9-1*, *var2-5, 092-004*
679 and representative lines overexpressing CTP_{SVR9}-infC in *svr9-1* or *092-004* background.

680

681 **Figure 4.** *SVR9* and *SVR9-like* genes in *Arabidopsis*. A, Gene models of three *Arabidopsis*
682 genes coding for putative prokaryotic type IF3 proteins. Gene models were drawn as in Fig.
683 2A. Numbers of nucleotides of each exon excluding the lengths of UTRs were labeled on top
684 of each exon. B, Transient expression of *SVR9-GFP*, *SVR9L1-GFP* or *GFP* alone in wild type
685 *Arabidopsis* leaf protoplasts. A single representative protoplast was shown for each
686 transformation. Merged images from *GFP* and chlorophyll channels were shown in the
687 “Merge” lane. BF, bright field. Bars, 10 μ m. C-D, Tissue expression patterns of *SVR9*.
688 Illustrated are *GUS* staining of 6-day-old (C) and 2-week-old (D) transgenic plants expressing
689 the transcriptional fusion of *P_{SVR9}:GUS*.

690

691 **Figure 5.** Genetic interactions between *var2*, *svr9-2* and *svr9II-1*. A-D, The first true leaves
692 of representative 2-week-old WT, *var2-5* and *var2-4* (A), *svr9II-1*, *svr9-2* and *svr9II-1 svr9-2*
693 double mutant (B), *svr9II-1 var2-5* double mutant, *svr9-2 var2-5* double mutant, and *svr9II-1*
694 *svr9-2 var2-5* triple mutant (C), *svr9II-1 var2-4* double mutant, *svr9-2 var2-4* double mutant
695 and *svr9II-1 svr9-2 var2-4* triple mutant (D). E-H, Quantitative comparison of leaf
696 variegation based on the frequency distributions of the pixel intensity values of leaf images
697 shown in A-D.

698

699 **Figure 6.** Functional redundancy of *SVR9* and *SVR9LI*. A, Overall phenotypes of 2-week-old
700 WT, *svr9II-1*, *svr9-1* and *svr9-1 svr9II-1/+*. B, Seed settings of WT and *svr9-1 svr9II-1/+*.
701 Developing siliques of WT and *svr9-1 svr9II-1/+* at the same stage were dissected and
702 photographed with a stereoscope. White arrows indicated the abolished embryos in *svr9-1*
703 *svr9II-1/+* silique. Bars, 2.5 mm. C, Overall phenotypes of 2-week-old WT, *svr9-1* and a
704 representative line overexpressing *SVR9LI* in the *svr9-1* background.

705

706 **Figure 7.** Leaf development phenotypes in *svr9-1*, *svr9II-1* and *svr9-1 svr9II-1/+* mutants. A,
707 Photographs of the third true leaves of representative 2-week-old WT, *svr9II-1*, *svr9-1* and
708 *svr9-1 svr9II-1/+*. Bars, 1 mm. B-D, Quantitative comparisons of leaf shapes in WT, *svr9II-1*,
709 *svr9-1* and *svr9-1 svr9II-1/+* based on the leaf dissection index ($\text{perimeter}^2/4\pi \times \text{leaf area}$) (B),
710 the number of teeth/leaf perimeter (C), and the tooth area/leaf area (D). All measurements
711 were performed on the third true leaves of 2-week-old plants. 10 leaves of each genotype
712 were included in the statistical analysis. Data were presented as mean \pm s.d. ***: $p < 0.001$. E,
713 Cross sections of the basal part of the first true leaves of 10-day-old WT, *svr9-1* and *svr9-1*
714 *svr9II-1/+*. Bars, 50 μm . F, Common cotyledon vein patterns observed in WT, *svr9-1* and
715 *svr9-1 svr9II-1/+*.

716

717 **Figure 8.** Repression of chloroplast translation alters *DR5:GUS* expression pattern. Images of
718 three representative cotyledons were shown for each genotype or treatment. A-C, Comparison
719 of *DR5:GUS* expression patterns in WT, *svr9-1* and *svr9-1 svr9II-1/+* backgrounds.

720 *DR5:GUS* activities were assayed in cotyledons of 6-day-old seedlings grown on solid 1/2
721 MS medium. D-F, Effects of chloroplast translation inhibitors on *DR5:GUS* expression. 6-
722 day-old wild type background *DR5:GUS* seedlings maintained in liquid 1/2 MS culture were
723 treated with 5 mM chloramphenicol, 5 mM spectinomycin or equal amounts of ethanol (mock
724 treatment) for 24 hours before assaying *DR5:GUS* activities. Bars, 1 mm.

725

726 **Figure 9.** Effects of auxin transport inhibitors on leaf margin development. A-B, WT, *svr9-1*
727 and *svr9-1 svr9II-1/+* were grown on solid 1/2 MS medium supplemented with 1 μM TIBA

728 (A), 1 μ M NPA (B) or equal amounts of DMSO (mock treatment) for 14 days. The third true
729 leaves from representative plants of each genotype were illustrated. Bars, 1 mm. C-D,
730 Quantification of the effects of TIBA (C) and NPA (D) on leaf shape by leaf dissection index
731 measurements. Data were presented as mean \pm s.d. **:0.001< p <0.01; ***: p <0.001.

732

733 **Figure 10.** Genetic interactions between *cuc2* mutants and *svr9-1*, *svr9ll-1* mutants. A,
734 Photographs of the third true leaves in representative 2-week-old WT, *cuc2-101*, *cuc2-1D*,
735 *svr9-1*, *cuc2-101 svr9-1*, *cuc2-1D svr9-1*, *svr9-1 svr9ll-1/+*, *cuc2-101 svr9-1 svr9ll-1/+*, and
736 *cuc2-1D svr9-1 svr9ll-1/+*. B-D, Quantitative comparisons of leaf margins of indicated
737 genotypes. Leaf margin quantifications were based on the leaf dissection index (B), the
738 number of teeth/leaf perimeter (C), and the tooth area/leaf area (D). All leaf shape parameters
739 were obtained as in Fig. 7. Data were presented as mean \pm s.d. ***: p <0.001.

740

741

742 **Tables**

743 **Table 1.** Quantification of cotyledon vein patterns in wild type, *svr9-1* and *svr9-1 svr9ll-1/+*.

744 Percentages of different types of areoles were indicated in the parentheses.

Genotype	Total*	Cotyledon vein patterns					
		Zero Areole	One Areole	Two Areoles	Three Areoles	Four Areoles	Five Areoles
WT	328	N.A.	N.A.	134 (40.8%)	135 (41.2%)	59 (18%)	N.A.
<i>svr9-1</i>	429	N.A.	13 (3%)	164 (38.2%)	183 (42.7%)	68 (15.9%)	1 (0.2%)
<i>svr9-1 svr9ll-1/+</i>	317	3 (1%)	67 (21.1%)	177 (55.8%)	69 (21.8%)	1 (0.3%)	N.A.

745 *Total number of cotyledons examined.

746

747

748 **Literature cited**

- 749 Aluru MR, Bae H, Wu D, Rodermel SR (2001) The *Arabidopsis immutans* mutation affects
750 plastid differentiation and the morphogenesis of white and green sectors in variegated
751 plants. *Plant Physiol* 127: 67-77
- 752 Bilsborough GD, Runions A, Barkoulas M, Jenkins HW, Hasson A, Galinha C, Laufs P, Hay
753 A, Prusinkiewicz P, Tsiantis M (2011) Model for the regulation of *Arabidopsis thaliana*
754 leaf margin development. *Proc Natl Acad Sci USA* 108: 3424-3429
- 755 Briggs GC, Osmont KS, Shindo C, Sibout R, Hardtke CS (2006) Unequal genetic
756 redundancies in *Arabidopsis*--a neglected phenomenon? *Trends Plant Sci* 11: 492-498
- 757 Byrne ME (2012) Making leaves. *Curr Opin Plant Biol* 15: 24-30
- 758 Cheng Y, Dai X, Zhao Y (2007) Auxin synthesized by the YUCCA flavin monooxygenases is
759 essential for embryogenesis and leaf formation in *Arabidopsis*. *Plant Cell* 19: 2430-2439
- 760 Chi W, Sun X, Zhang L (2013) Intracellular signaling from plastid to nucleus. *Annu Rev Plant*
761 *Biol* 64: 559-582
- 762 Clough SJ, Bent AF (1998). Floral dip: A simplified method for *Agrobacterium*-mediated
763 transformation of *Arabidopsis thaliana*. *Plant J* 16: 735-743
- 764 Dyall SD, Brown MT, Johnson PJ (2004) Ancient invasions: from endosymbionts to
765 organelles. *Science* 304: 253-257
- 766 Fleischmann TT, Scharff LB, Alkatib S, Hasdorf S, Schöttler MA, Bock R (2011)
767 Nonessential plastid-encoded ribosomal proteins in tobacco: a developmental role for
768 plastid translation and implications for reductive genome evolution. *Plant Cell* 23: 3137-
769 3155
- 770 Galvez-Valdivieso G, Mullineaux PM (2010) The role of reactive oxygen species in signalling
771 from chloroplasts to the nucleus. *Physiol Plant* 138: 430-39
- 772 Gray JC, Sullivan JA, Wang JH, Jerome CA, MacLean D (2003) Coordination of plastid and
773 nuclear gene expression. *Philos Trans R Soc Lond B* 358: 135-44
- 774 Hricová A, Quesada V, Micol JL (2006) The SCABRA3 nuclear gene encodes the plastid
775 RpoTp RNA polymerase, which is required for chloroplast biogenesis and mesophyll
776 cell proliferation in *Arabidopsis*. *Plant Physiol* 141: 942-956
- 777 Jefferson RA (1987) Assaying chimeric genes in plants: the GUS gene fusion system. *Plant*
778 *Mol Biol Rep* 5: 387-405
- 779 Jensen PE, Leister D (2014) Chloroplast evolution, structure and functions. *F1000Prime Rep*
780 6: 40
- 781 Josse EM, Simkin AJ, Gaffé J, Labouré AM, Kuntz M, Carol P (2000) A plastid terminal
782 oxidase associated with carotenoid desaturation during chromoplast differentiation. *Plant*
783 *Physiol* 123: 1427-1436

784 Kawamura E1, Horiguchi G, Tsukaya H. (2010) Mechanisms of leaf tooth formation in
785 *Arabidopsis*. Plant J 62:429-441

786 Kindgren P, Kremnev D, Blanco NE, de Dios Barajas López J, Fernández AP, Tellgren-Roth
787 C, Kleine T, Small I, Strand A (2012) The plastid redox insensitive 2 mutant of
788 *Arabidopsis* is impaired in PEP activity and high light-dependent plastid redox signalling
789 to the nucleus. Plant J 70: 279-291

790 Koussevitzky S, Nott A, Mockler TC, Hong F, Sachetto-Martins G, Surpin M, Lim J, Mittler
791 R, Chory J (2007) Signals from chloroplasts converge to regulate nuclear gene
792 expression. Science 316: 715-719

793 Larue CT, Wen J, Walker JC (2009) A microRNA-transcription factor module regulates lateral
794 organ size and patterning in *Arabidopsis*. Plant J 58: 450-463

795 Lee KP, Kim C, Landgraf F, Apel K (2007) EXECUTER1- and EXECUTER2-dependent
796 transfer of stress-related signals from the plastid to the nucleus of *Arabidopsis thaliana*.
797 Proc Natl Acad Sci USA 104: 10270-10275

798 Leister D (2003) Chloroplast research in the genomic age. Trends Genet 19: 47-56

799 Leister D (2012) Retrograde signaling in plants: from simple to complex scenarios. Front
800 Plant Sci 3: 135

801 Lichtenthaler HK (1987) Chlorophylls, carotenoids: pigments of photosynthetic
802 biomembranes. Methods Enzymol 148: 350-382

803 Liu X, Yu F, Rodermel S (2010a) *Arabidopsis* chloroplast FtsH, *var2* and suppressors of *var2*
804 leaf variegation: a review. J Integr Plant Biol 52: 750-761

805 Liu X, Yu F, Rodermel S (2010b) An *Arabidopsis* pentatricopeptide repeat protein,
806 SUPPRESSOR OF VARIATION7, is required for FtsH-mediated chloroplast
807 biogenesis. Plant Physiol 154: 1588-1601

808 Liu X, Rodermel SR, Yu F (2010c) A *var2* leaf variegation suppressor locus, SUPPRESSOR
809 OF VARIATION3, encodes a putative chloroplast translation elongation factor that is
810 important for chloroplast development in the cold. BMC Plant Biol 10: 287

811 Liu X, Zheng M, Wang R, Wang R, An L, Rodermel SR, Yu F (2013) Genetic interactions
812 reveal that specific defects of chloroplast translation are associated with the suppression
813 of *var2*-mediated leaf variegation. J Integr Plant Biol 55: 979-993

814 Lomakin IB, Shirokikh NE, Yusupov MM, Hellen CU, Pestova TV (2006) The fidelity of
815 translation initiation: reciprocal activities of eIF1, IF3 and YciH. EMBO J 25: 196-210

816 Lukowitz W, Gillmor CS, Scheible WR (2000) Positional cloning in *Arabidopsis*: why it feels
817 good to have a genome initiative working for you. Plant Physiol 123: 795-805

818 Mandel MA, Feldmann KA, Herrera-Estrella L, Rocha-Sosa M, León P (1996) *CLA1*, a novel
819 gene required for chloroplast development, is highly conserved in evolution. Plant J 9:
820 649-658

-
- 821 Milon P, Konevega AL, Gualerzi CO, Rodnina MV (2008) Kinetic checkpoint at a late step in
822 translation initiation. *Mol Cell* 30: 712-720
- 823 Miura E, Kato Y, Matsushima R, Albrecht V, Laalami S, Sakamoto W (2007) The balance
824 between protein synthesis and degradation in chloroplasts determines leaf variegation in
825 *Arabidopsis yellow variegated* mutants. *Plant Cell* 19: 1313-1328
- 826 Mochizuki N, Tanaka R, Tanaka A, Masuda T, Nagatani A (2008) The steady-state level of
827 Mg-protoporphyrin IX is not a determinant of plastid-to-nucleus signaling in
828 *Arabidopsis*. *Proc Natl Acad Sci USA* 105: 15184-15189
- 829 Moulin M, McCormac AC, Terry MJ, Smith AG (2008) Tetrapyrrole profiling in *Arabidopsis*
830 seedlings reveals that retrograde plastid nuclear signaling is not due to Mg-
831 protoporphyrin IX accumulation. *Proc Natl Acad Sci USA* 105: 15178-15183
- 832 Nesbit AD, Whippo C, Hangarter RP, Kehoe DM (2015) Translation initiation factor 3
833 families: what are their roles in regulating cyanobacterial and chloroplast gene
834 expression? *Photosynth Res* 126: 147-159
- 835 Nikovics K, Blein T, Peaucelle A, Ishida T, Morin H, Aida M, Laufs P (2006) The balance
836 between the *MIR164A* and *CUC2* genes controls leaf margin serration in *Arabidopsis*.
837 *Plant Cell* 18: 2929-2945
- 838 Nott A, Jung HS, Koussevitzky S, Chory J (2006) Plastid-to-nucleus retrograde signaling.
839 *Annu Rev Plant Biol* 57: 739-759
- 840 Pesaresi P, Hertle A, Pribil M, Kleine T, Wagner R, Strissel H, Ichnatowicz A, Bonardi V,
841 Scharfenberg M, Schneider A, Pfannschmidt T, Leister D (2009) *Arabidopsis* STN7
842 kinase provides a link between short- and long-term photosynthetic acclimation. *Plant*
843 *Cell* 21: 2402-2423
- 844 Pesaresi P, Masiero S, Eubel H, Braun HP, Bhushan S, Glaser E, Salamini F, Leister D (2006)
845 Nuclear photosynthetic gene expression is synergistically modulated by rates of protein
846 synthesis in chloroplasts and mitochondria. *Plant Cell* 18: 970-991
- 847 Putarjunan A, Liu X, Nolan T, Yu F, Rodermel S (2013) Understanding chloroplast biogenesis
848 using second-site suppressors of *immutans* and *var2*. *Photosynth Res* 116: 437-453
- 849 Qi Y, Zhao J, An R, Zhang J, Liang S, Shao J, Liu X, An L, Yu F (2015) Mutations in
850 circularly permuted GTPase family genes *AtNOA1/RIF1/SVR10* and *BPG2* suppress
851 *var2*-mediated leaf variegation in *Arabidopsis thaliana*. *Photosynth Res* DOI:
852 10.1007/s11120-015-0195-9
- 853 Ramel F, Birtic S, Ginies C, Soubigou-Taconnat L, Triantaphylidès C, Havaux M (2012)
854 Carotenoid oxidation products are stress signals that mediate gene responses to single to
855 oxygen in plants. *Proc Natl Acad Sci USA* 109: 5535-5540
- 856 Reiter RS, Coomber SA, Bourett TM, Bartley GE, Scolnik PA (1994) Control of leaf and
857 chloroplast development by the *Arabidopsis* gene *pale cress*. *Plant Cell* 6: 1253-1264

858 Royer DL, McElwain JC, Adams JM, Wilf P (2008) Sensitivity of leaf size and shape to
859 climate within *Acer rubrum* and *Quercus kelloggii*. *New Phytol* 179: 808-817

860 Sacerdot C, Fayat G, Dessen P, Springer M, Plumbridge JA, Grunberg-Manago M, Blanquet S
861 (1982) Sequence of a 1.26-kb DNA fragment containing the structural gene for *E.coli*
862 initiation factor IF3: presence of an AUU initiator codon. *EMBO J* 1: 311-315

863 Saini G, Meskauskiene R, Pijacka W, Roszak P, Sjögren LL, Clarke AK, Straus M, Apel K
864 (2011) 'happy on norflurazon' (*hon*) mutations implicate perturbation of plastid
865 homeostasis with activating stress acclimatization and changing nuclear gene expression
866 in norflurazon-treated seedlings. *Plant J* 65: 690-702

867 Scarpella E, Marcos D, Friml J, Berleth T (2006) Control of leaf vascular patterning by polar
868 auxin transport. *Genes Dev* 20: 1012-1027

869 Sieburth LE (1999) Auxin is required for leaf vein pattern in *Arabidopsis*. *Plant Physiol* 121:
870 1179-1190

871 Sun X, Feng P, Xu X, Guo H, Ma J, Chi W, Lin R, Lu C, Zhang L (2011) A chloroplast
872 envelope-bound PHD transcription factor mediates chloroplast signals to the nucleus.
873 *Nat Commun* 2: 477

874 Susek RE, Ausubel FM, Chory J (1993) Signal transduction mutants of *Arabidopsis* uncouple
875 nuclear *CAB* and *RBCS* gene expression from chloroplast development. *Cell* 74: 787-799

876 Tiller N, Bock R (2014) The translational apparatus of plastids and its role in plant
877 development. *Mol Plant* 7: 1105-1120

878 Ulmasov T, Murfett J, Hagen G, Guilfoyle TJ (1997) Aux/IAA proteins repress expression of
879 reporter genes containing natural and highly active synthetic auxin response elements.
880 *Plant Cell* 9: 1963-1971

881 Wagner D, Przybyla D, Op den Camp R, Kim C, Landgraf F, Lee KP, Würsch M, Laloï C,
882 Nater M, Hideg E, Apel K. (2004) The genetic basis of singlet oxygen-induced stress
883 responses of *Arabidopsis thaliana*. *Science* 306: 183-185

884 Wilson PB, Estavillo GM, Field KJ, Pornsiriwong W, Carroll AJ, Howell KA, Woo NS, Lake
885 JA, Smith SM, Harvey Millar A, von Caemmerer S, Pogson BJ (2009) The
886 nucleotidase/phosphatase SAL1 is a negative regulator of drought tolerance in
887 *Arabidopsis*. *Plant J* 58: 299-317

888 Woodson JD, Chory J (2008) Coordination of gene expression between organellar and nuclear
889 genomes. *Nat Rev Genet* 9: 383-395

890 Woodson JD, Chory J (2012) Organelle signaling: how stressed chloroplasts communicate
891 with the nucleus. *Curr Biol* 22: R690-R692

892 Xiang C, Han P, Lutziger I, Wang K, Oliver DJ (1999) A mini binary vector series for plant
893 transformation. *Plant Mol Biol* 40: 711-717

-
- 894 Xiao Y, Savchenko T, Baidoo EE, Chehab WE, Hayden DM, Tolstikov V, Corwin JA,
895 Kliebenstein DJ, Keasling JD, Dehesh K (2012) Retrograde signaling by the plastidial
896 metabolite MEcPP regulates expression of nuclear stress-response genes. *Cell* 149:
897 1525-1535
- 898 Yoo SD, Cho YH, Sheen J (2007) *Arabidopsis* mesophyll protoplasts: a versatile cell system
899 for transient gene expression analysis. *Nat Protoc* 2: 1565-1572
- 900 Yu F, Liu X, Alsheikh M, Park S, Rodermel S (2008) Mutations in *SUPPRESSOR OF*
901 *VARIEGATION1*, a factor required for normal chloroplast translation, suppress *var2*-
902 mediated leaf variegation in *Arabidopsis*. *Plant Cell* 20: 1786-1804
- 903 Yu F, Park S, Rodermel SR (2004) The *Arabidopsis* FtsH metalloprotease gene family:
904 interchangeability of subunits in chloroplast oligomeric complexes. *Plant J* 37: 864-876
- 905 Yu F, Park S, Rodermel SR (2005) Functional redundancy of AtFtsH metalloproteases in
906 thylakoid membrane complexes. *Plant Physiol* 138: 1957-1966
- 907 Yu F, Park SS, Liu X, Foudree A, Fu A, Powikrowska M, Khrouchtchova A, Jensen PE,
908 Kriger JN, Gray GR, Rodermel SR (2011) *SUPPRESSOR OF VARIEGATION4*, a new
909 *var2* suppressor locus, encodes a pioneer protein that is required for chloroplast
910 biogenesis. *Mol Plant*

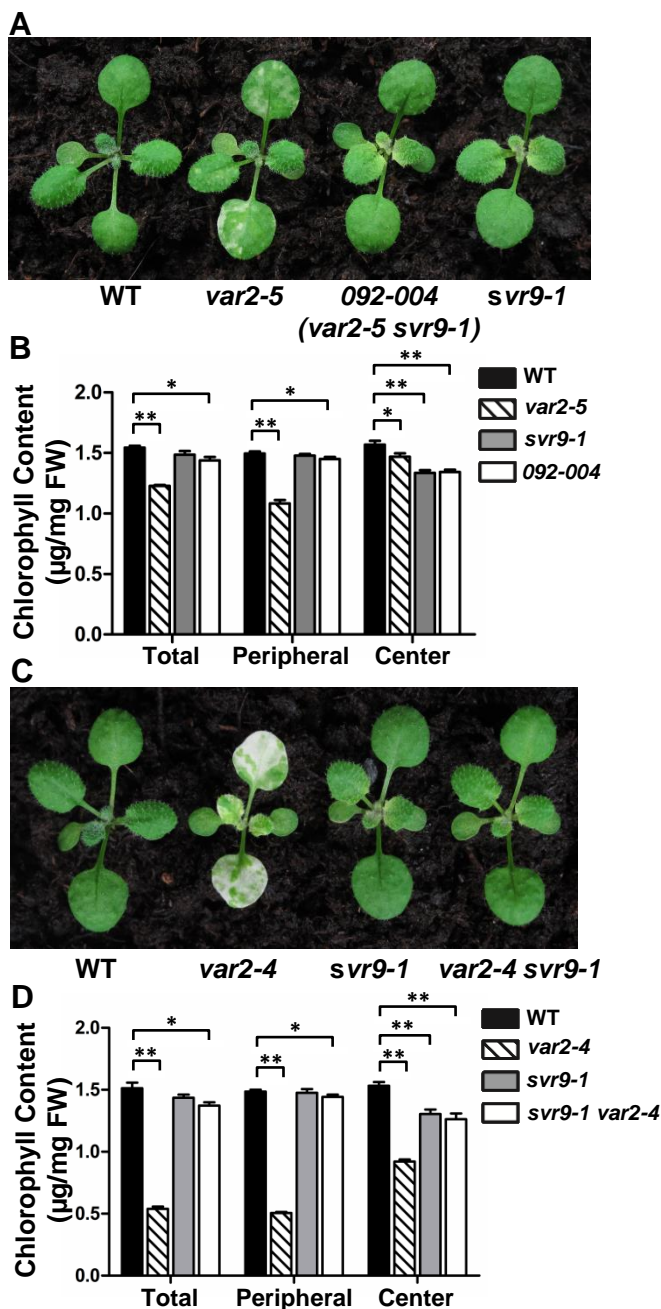


Figure 1. Suppression of *var2* leaf variegation by *svr9-1*. A, Representative 15-day-old wild type (WT), *var2-5*, *092-004* (*var2-5 svr9-1*), and *svr9-1* plants. C, Representative 15-day-old WT, *var2-4*, *svr9-1*, and *var2-4 svr9-1* double mutant. B and D, Chlorophyll contents of indicated tissues in plants shown in A and C, respectively. Total: entire rosettes excluding the cotyledons; Peripheral: the first two true leaves; Center: rosettes excluding the cotyledons and the first two true leaves. Chlorophyll measurements were normalized on a fresh tissue weight basis. Data were presented as mean \pm standard deviation (s.d.) of three biological replicates. *: $0.01 < p < 0.05$; **: $p < 0.01$.

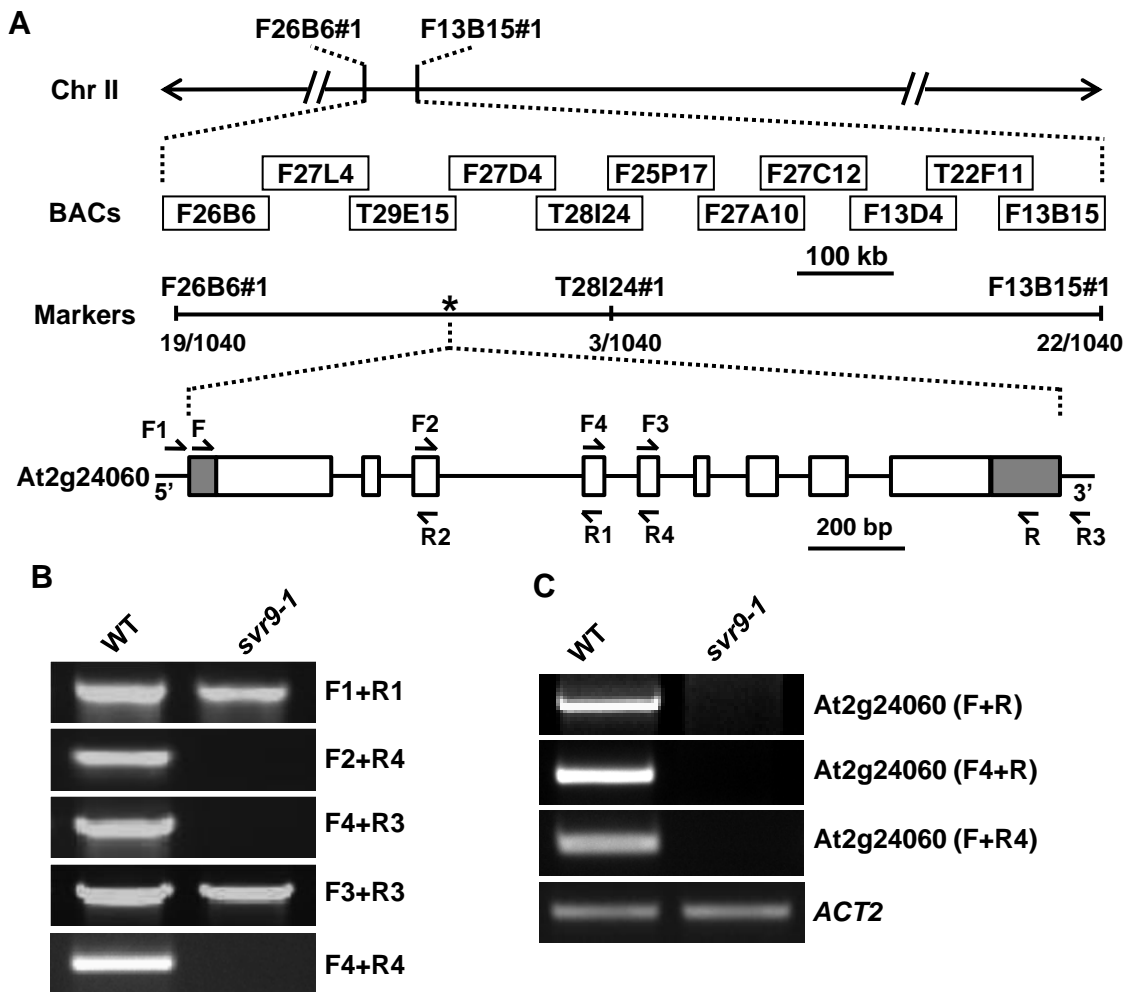


Figure 2. Cloning of *SVR9*. **A**, Schematic representation of the positional cloning procedure used to identify *svr9-1* mutation. Primers of the molecular markers designed in this study were listed in Supplemental Table S2. A total of 570 F₂ plants (1140 chromosomes) were used in fine mapping. Numbers of recombinants were marked under each molecular marker. The asterisk indicated the position of *SVR9* (*At2g24060*). In the gene model, boxes represent exons and lines represent introns. 5' and 3' untranslated regions (UTRs) were shaded. Arrows represent the positions of the primers used in **B** and **C**. **B**, PCR analyses using various primer combinations indicated that *At2g24060* genomic regions were disrupted in *svr9-1*. **C**, Semi-quantitative RT-PCR analyses of the accumulations of *SVR9* transcripts in wild type and *svr9-1* using indicated primer combinations. Expression of *ACT2* was used as an internal control.

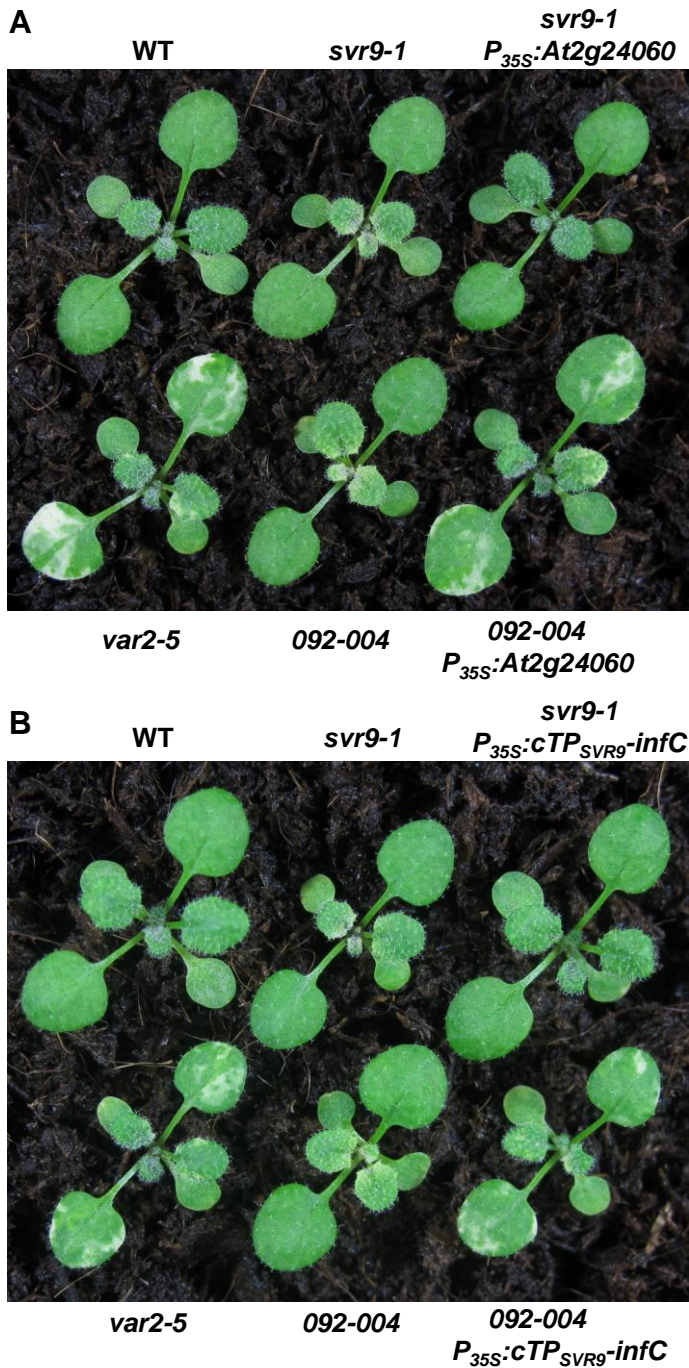


Figure 3. Complementation of *svr9-1* and *092-004*. A, Leaf color phenotypes of two-week-old WT, *svr9-1*, *var2-5*, *092-004* and representative lines overexpressing *At2g24060* in *svr9-1* or *092-004* background. B, Leaf color phenotypes of two-week-old WT, *svr9-1*, *var2-5*, *092-004* and representative lines overexpressing *CTP_{SVR9}-infC* in *svr9-1* or *092-004* background.

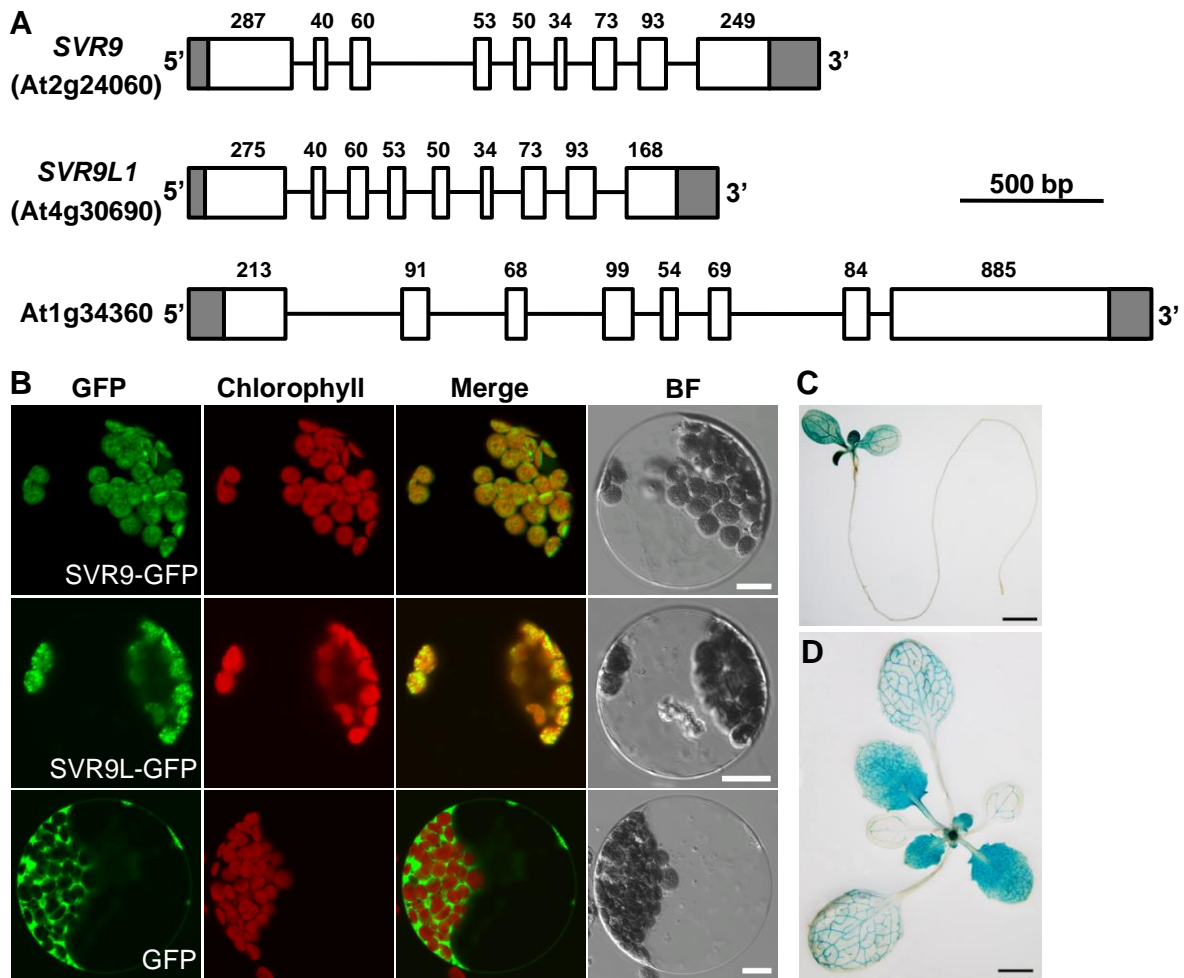


Figure 4. *SVR9* and *SVR9*-like genes in *Arabidopsis*. **A**, Gene models of three *Arabidopsis* genes coding for putative prokaryotic type IF3 proteins. Gene models were drawn as in Fig. 2A. Numbers of nucleotides of each exon excluding the lengths of UTRs were labeled on top of each exon. **B**, Transient expression of *SVR9*-GFP, *SVR9L1*-GFP or GFP alone in wild type *Arabidopsis* leaf protoplasts. A single representative protoplast was shown for each transformation. Merged images from GFP and chlorophyll channels were shown in the “Merge” lane. BF, bright field. Bars, 10 μ m. **C-D**, Tissue expression patterns of *SVR9*. Illustrated are GUS staining of 6-day-old (**C**) and 2-week-old (**D**) transgenic plants expressing the transcriptional fusion of $P_{SVR9}:GUS$.

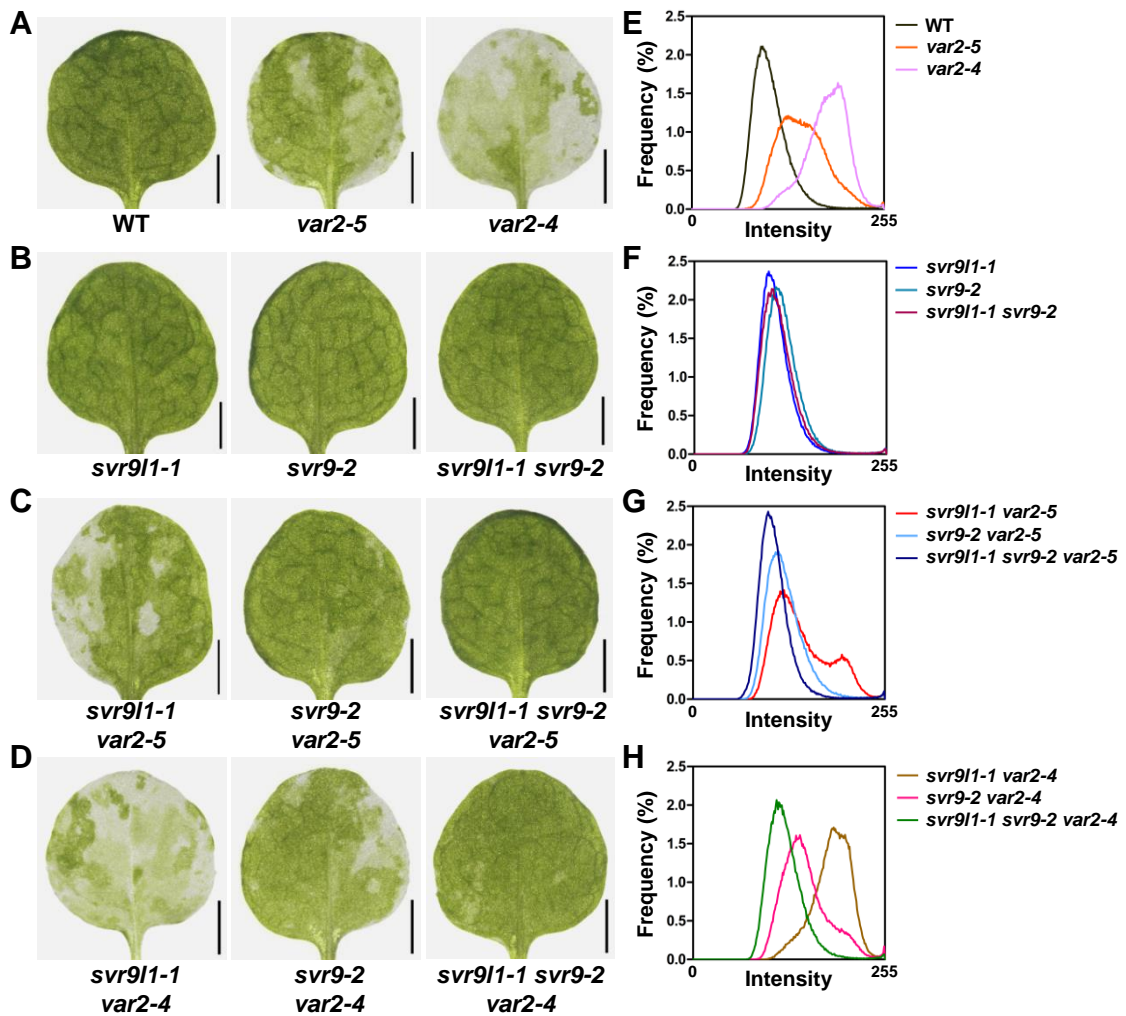


Figure 5. Genetic interactions between *var2*, *svr9-2* and *svr9/1-1*. A-D, The first true leaves of representative 2-week-old WT, *var2-5* and *var2-4* (A), *svr9/1-1*, *svr9-2* and *svr9/1-1 svr9-2* double mutant (B), *svr9/1-1 var2-5* double mutant, *svr9-2 var2-5* double mutant, and *svr9/1-1 svr9-2 var2-5* triple mutant (C), *svr9/1-1 var2-4* double mutant, *svr9-2 var2-4* double mutant and *svr9/1-1 svr9-2 var2-4* triple mutant (D). E-H, Quantitative comparison of leaf variegation based on the frequency distributions of the pixel intensity values of leaf images shown in A-D.

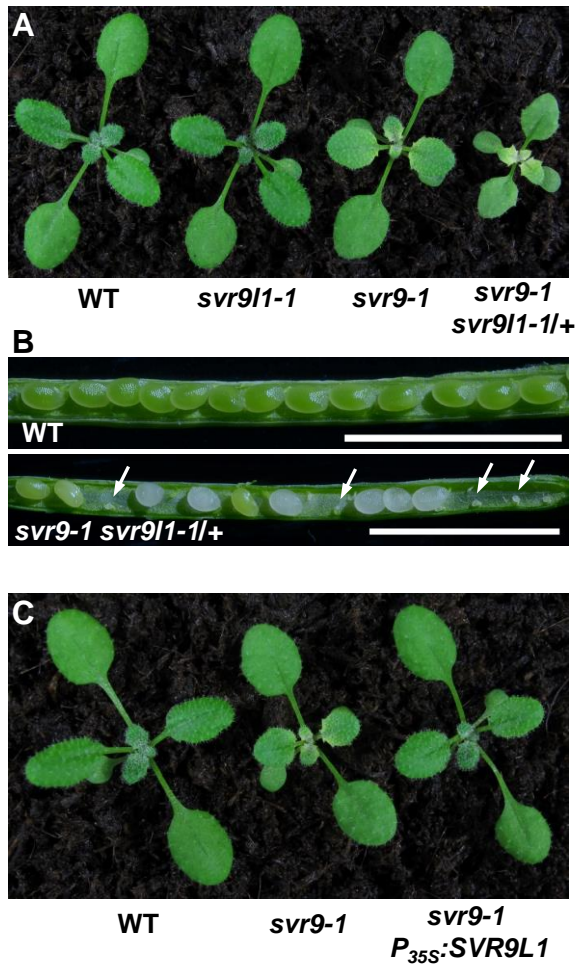


Figure 6. Functional redundancy of *SVR9* and *SVR9L1*. A, Overall phenotypes of 2-week-old WT, *svr9l1-1*, *svr9-1* and *svr9-1 svr9l1-1/+*. B, Seed settings of WT and *svr9-1 svr9l1-1/+*. Developing siliques of WT and *svr9-1 svr9l1-1/+* at the same stage were dissected and photographed with a stereoscope. White arrows indicated the abolished embryos in *svr9-1 svr9l1-1/+* silique. Bars, 2.5 mm. C, Overall phenotypes of 2-week-old WT, *svr9-1* and a representative line overexpressing *SVR9L1* in the *svr9-1* background.

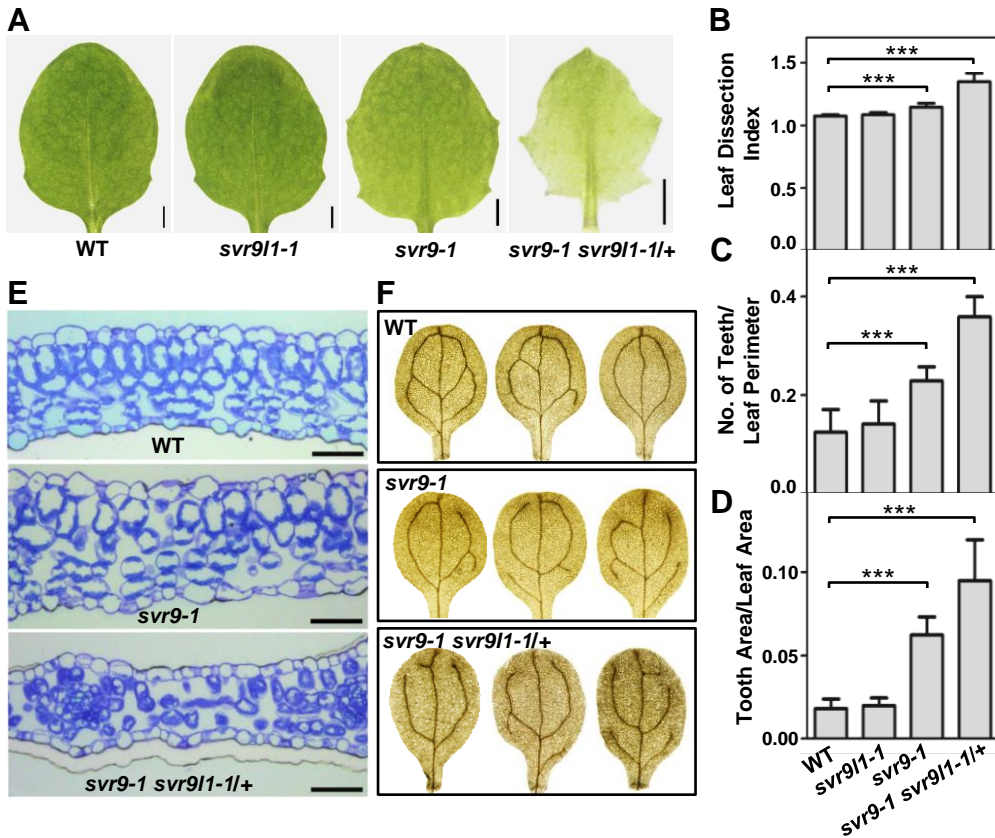


Figure 7. Leaf development phenotypes in *svr9-1*, *svr9/1-1* and *svr9-1 svr9/1-1/+* mutants. A, Photographs of the third true leaves of representative 2-week-old WT, *svr9/1-1*, *svr9-1* and *svr9-1 svr9/1-1/+*. Bars, 1 mm. B-D, Quantitative comparisons of leaf shapes in WT, *svr9/1-1*, *svr9-1* and *svr9-1 svr9/1-1/+* based on the leaf dissection index ($\text{perimeter}^2/4\pi \times \text{leaf area}$) (B), the number of teeth/leaf perimeter (C), and the tooth area/leaf area (D). All measurements were performed on the third true leaves of 2-week-old plants. 10 leaves of each genotype were included in the statistical analysis. Data were presented as mean \pm s.d. ***: $p < 0.001$. E, Cross sections of the basal part of the first true leaves of 10-day-old WT, *svr9-1* and *svr9-1 svr9/1-1/+*. Bars, 50 μm . F, Common cotyledon vein patterns observed in WT, *svr9-1* and *svr9-1 svr9/1-1/+*.

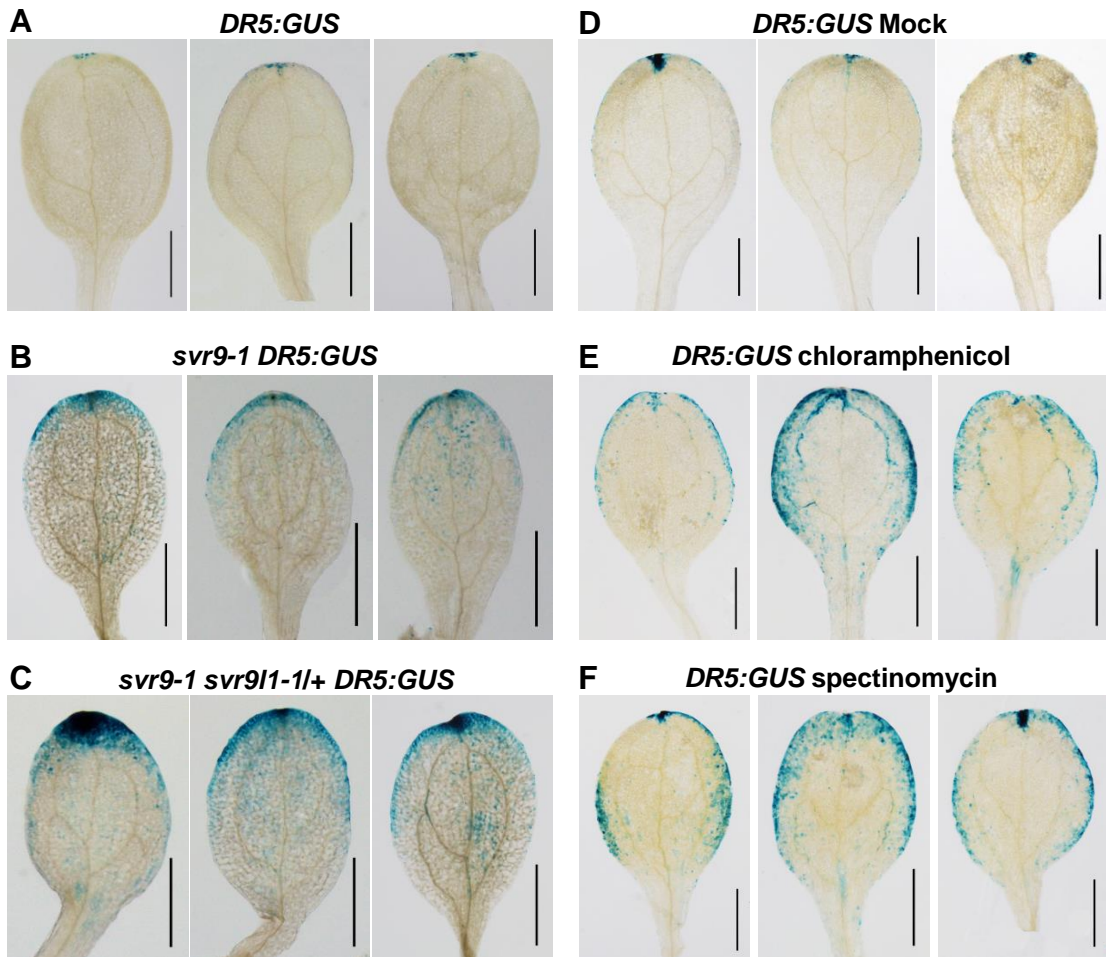


Figure 8. Repression of chloroplast translation alters *DR5:GUS* expression pattern. Images of three representative cotyledons were shown for each genotype or treatment. A-C, Comparison of *DR5:GUS* expression patterns in WT, *svr9-1* and *svr9-1 svr9I1-1/+* backgrounds. *DR5:GUS* activities were assayed in cotyledons of 6-day-old seedlings grown on solid 1/2 MS medium. D-F, Effects of chloroplast translation inhibitors on *DR5:GUS* expression. 6-day-old wild type background *DR5:GUS* seedlings maintained in liquid 1/2 MS culture were treated with 5 mM chloramphenicol, 5 mM spectinomycin or equal amounts of ethanol (mock treatment) for 24 hours before assaying *DR5:GUS* activities. Bars, 1 mm.

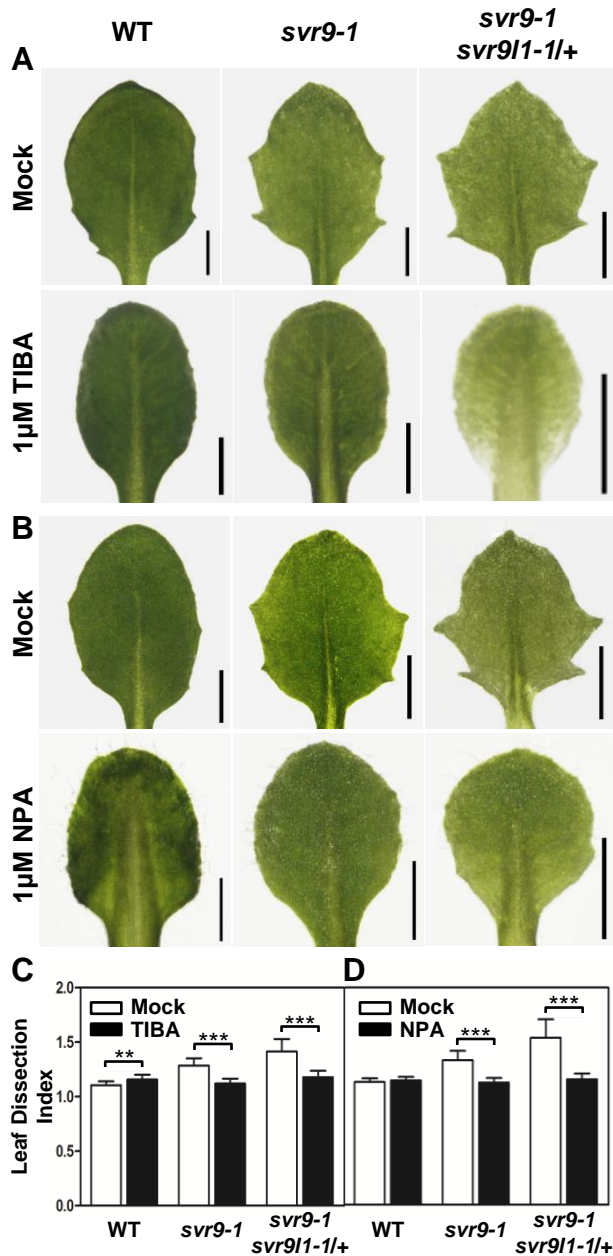


Figure 9. Effects of auxin transport inhibitors on leaf margin development. A-B, WT, *svr9-1* and *svr9-1 svr9/1-1/+* were grown on solid 1/2 MS medium supplemented with 1 μ M TIBA (A), 1 μ M NPA (B) or equal amounts of DMSO (mock treatment) for 14 days. The third true leaves from representative plants of each genotype were illustrated. Bars, 1 mm. C-D, Quantification of the effects of TIBA (C) and NPA (D) on leaf shape by leaf dissection index measurements. Data were presented as mean \pm s.d. **: $0.001 < p < 0.01$; ***: $p < 0.001$.

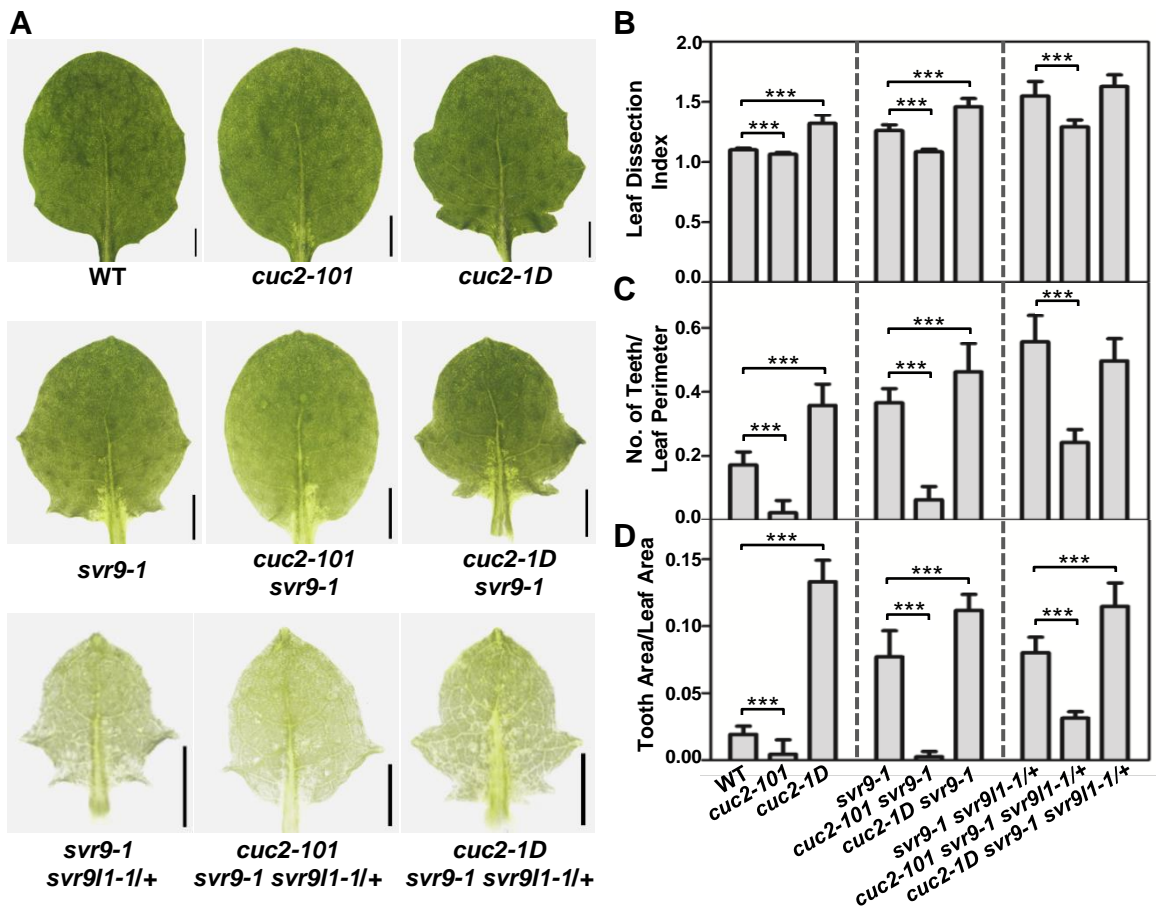


Figure 10. Genetic interactions between *cuc2* mutants and *svr9-1*, *svr9l1-1* mutants. A, Photographs of the third true leaves in representative 2-week-old WT, *cuc2-101*, *cuc2-1D*, *svr9-1*, *cuc2-101 svr9-1*, *cuc2-1D svr9-1*, *svr9-1 svr9l1-1/+*, *cuc2-101 svr9-1 svr9l1-1/+*, and *cuc2-1D svr9-1 svr9l1-1/+*. B-D, Quantitative comparisons of leaf margins of indicated genotypes. Leaf margin quantifications were based on the leaf dissection index (B), the number of teeth/leaf perimeter (C), and the tooth area/leaf area (D). All leaf shape parameters were obtained as in Fig. 7. Data were presented as mean \pm s.d. ***: $p < 0.001$.

Parsed Citations

Aluru MR, Bae H, Wu D, Rodermeil SR (2001) The Arabidopsis immutans mutation affects plastid differentiation and the morphogenesis of white and green sectors in variegated plants. Plant Physiol 127: 67-77

Pubmed: [Author and Title](#)

CrossRef: [Author and Title](#)

Google Scholar: [Author Only](#) [Title Only](#) [Author and Title](#)

Bilsborough GD, Runions A, Barkoulas M, Jenkins HW, Hasson A, Galinha C, Laufs P, Hay A, Prusinkiewicz P, Tsiantis M (2011) Model for the regulation of Arabidopsis thaliana leaf margin development. Proc Natl Acad Sci USA 108: 3424-3429

Pubmed: [Author and Title](#)

CrossRef: [Author and Title](#)

Google Scholar: [Author Only](#) [Title Only](#) [Author and Title](#)

Briggs GC, Osmont KS, Shindo C, Sibout R, Hardtke CS (2006) Unequal genetic redundancies in Arabidopsis--a neglected phenomenon? Trends Plant Sci 11: 492-498

Pubmed: [Author and Title](#)

CrossRef: [Author and Title](#)

Google Scholar: [Author Only](#) [Title Only](#) [Author and Title](#)

Byrne ME (2012) Making leaves. Curr Opin Plant Biol 15: 24-30

Pubmed: [Author and Title](#)

CrossRef: [Author and Title](#)

Google Scholar: [Author Only](#) [Title Only](#) [Author and Title](#)

Cheng Y, Dai X, Zhao Y (2007) Auxin synthesized by the YUCCA flavin monooxygenases is essential for embryogenesis and leaf formation in Arabidopsis. Plant Cell 19: 2430-2439

Pubmed: [Author and Title](#)

CrossRef: [Author and Title](#)

Google Scholar: [Author Only](#) [Title Only](#) [Author and Title](#)

Chi W, Sun X, Zhang L (2013) Intracellular signaling from plastid to nucleus. Annu Rev Plant Biol 64: 559-582

Pubmed: [Author and Title](#)

CrossRef: [Author and Title](#)

Google Scholar: [Author Only](#) [Title Only](#) [Author and Title](#)

Clough SJ, Bent AF (1998). Floral dip: A simplified method for Agrobacterium-mediated transformation of Arabidopsis thaliana. Plant J 16: 735-743

Pubmed: [Author and Title](#)

CrossRef: [Author and Title](#)

Google Scholar: [Author Only](#) [Title Only](#) [Author and Title](#)

Dyall SD, Brown MT, Johnson PJ (2004) Ancient invasions: from endosymbionts to organelles. Science 304: 253-257

Pubmed: [Author and Title](#)

CrossRef: [Author and Title](#)

Google Scholar: [Author Only](#) [Title Only](#) [Author and Title](#)

Fleischmann TT, Scharff LB, Alkatib S, Hasdorf S, Schöttler MA, Bock R (2011) Nonessential plastid-encoded ribosomal proteins in tobacco: a developmental role for plastid translation and implications for reductive genome evolution. Plant Cell 23: 3137-3155

Pubmed: [Author and Title](#)

CrossRef: [Author and Title](#)

Google Scholar: [Author Only](#) [Title Only](#) [Author and Title](#)

Galvez-Valdivieso G, Mullineaux PM (2010) The role of reactive oxygen species in signalling from chloroplasts to the nucleus. Physiol Plant 138: 430-39

Pubmed: [Author and Title](#)

CrossRef: [Author and Title](#)

Google Scholar: [Author Only](#) [Title Only](#) [Author and Title](#)

Gray JC, Sullivan JA, Wang JH, Jerome CA, MacLean D (2003) Coordination of plastid and nuclear gene expression. Philos Trans R Soc Lond B 358: 135-44

Pubmed: [Author and Title](#)

CrossRef: [Author and Title](#)

Google Scholar: [Author Only](#) [Title Only](#) [Author and Title](#)

Hricová A, Quesada V, Micol JL (2006) The SCABRA3 nuclear gene encodes the plastid RpoTp RNA polymerase, which is required for chloroplast biogenesis and mesophyll cell proliferation in Arabidopsis. Plant Physiol 141: 942-956

Pubmed: [Author and Title](#)

CrossRef: [Author and Title](#)

Google Scholar: [Author Only](#) [Title Only](#) [Author and Title](#)

Jefferson RA (1987) Assaying chimeric genes in plants: the GUS gene fusion system. Plant Mol Biol Rep 5: 387-405

Pubmed: [Author and Title](#)

CrossRef: [Author and Title](#)

Google Scholar: [Author Only](#) [Title Only](#) [Author and Title](#)

Jensen PE, Leister D (2014) Chloroplast evolution, structure and functions. F1000Prime Rep 6: 40

Pubmed: [Author and Title](#)

CrossRef: [Author and Title](#)

Google Scholar: [Author Only](#) [Title Only](#) [Author and Title](#)

Josse EM, Simkin AJ, Gaffé J, Labouré AM, Kuntz M, Carol P (2000) A plastid terminal oxidase associated with carotenoid desaturation during chromoplast differentiation. *Plant Physiol* 123: 1427-1436

Pubmed: [Author and Title](#)

CrossRef: [Author and Title](#)

Google Scholar: [Author Only](#) [Title Only](#) [Author and Title](#)

Kawamura E1, Horiguchi G, Tsukaya H. (2010) Mechanisms of leaf tooth formation in Arabidopsis. *Plant J* 62:429-441

Pubmed: [Author and Title](#)

CrossRef: [Author and Title](#)

Google Scholar: [Author Only](#) [Title Only](#) [Author and Title](#)

Kindgren P, Kremnev D, Blanco NE, de Dios Barajas López J, Fernández AP, Tellgren-Roth C, Kleine T, Small I, Strand A (2012) The plastid redox insensitive 2 mutant of Arabidopsis is impaired in PEP activity and high light-dependent plastid redox signalling to the nucleus. *Plant J* 70: 279-291

Pubmed: [Author and Title](#)

CrossRef: [Author and Title](#)

Google Scholar: [Author Only](#) [Title Only](#) [Author and Title](#)

Koussevitzky S, Nott A, Mockler TC, Hong F, Sachetto-Martins G, Surpin M, Lim J, Mittler R, Chory J (2007) Signals from chloroplasts converge to regulate nuclear gene expression. *Science* 316: 715-719

Pubmed: [Author and Title](#)

CrossRef: [Author and Title](#)

Google Scholar: [Author Only](#) [Title Only](#) [Author and Title](#)

Larue CT, Wen J, Walker JC (2009) A microRNA-transcription factor module regulates lateral organ size and patterning in Arabidopsis. *Plant J* 58: 450-463

Pubmed: [Author and Title](#)

CrossRef: [Author and Title](#)

Google Scholar: [Author Only](#) [Title Only](#) [Author and Title](#)

Lee KP, Kim C, Landgraf F, Apel K (2007) EXECUTER1- and EXECUTER2-dependent transfer of stress-related signals from the plastid to the nucleus of Arabidopsis thaliana. *Proc Natl Acad Sci USA* 104: 10270-10275

Pubmed: [Author and Title](#)

CrossRef: [Author and Title](#)

Google Scholar: [Author Only](#) [Title Only](#) [Author and Title](#)

Leister D (2003) Chloroplast research in the genomic age. *Trends Genet* 19: 47-56

Pubmed: [Author and Title](#)

CrossRef: [Author and Title](#)

Google Scholar: [Author Only](#) [Title Only](#) [Author and Title](#)

Leister D (2012) Retrograde signaling in plants: from simple to complex scenarios. *Front Plant Sci* 3: 135

Pubmed: [Author and Title](#)

CrossRef: [Author and Title](#)

Google Scholar: [Author Only](#) [Title Only](#) [Author and Title](#)

Lichtenthaler HK (1987) Chlorophylls, carotenoids: pigments of photosynthetic biomembranes. *Methods Enzymol* 148: 350-382

Pubmed: [Author and Title](#)

CrossRef: [Author and Title](#)

Google Scholar: [Author Only](#) [Title Only](#) [Author and Title](#)

Liu X, Yu F, Rodermeil S (2010a) Arabidopsis chloroplast FtsH, var2 and suppressors of var2 leaf variegation: a review. *J Integr Plant Biol* 52: 750-761

Pubmed: [Author and Title](#)

CrossRef: [Author and Title](#)

Google Scholar: [Author Only](#) [Title Only](#) [Author and Title](#)

Liu X, Yu F, Rodermeil S (2010b) An Arabidopsis pentatricopeptide repeat protein, SUPPRESSOR OF VARIATION7, is required for FtsH-mediated chloroplast biogenesis. *Plant Physiol* 154: 1588-1601

Pubmed: [Author and Title](#)

CrossRef: [Author and Title](#)

Google Scholar: [Author Only](#) [Title Only](#) [Author and Title](#)

Liu X, Rodermeil SR, Yu F (2010c) A var2 leaf variegation suppressor locus, SUPPRESSOR OF VARIATION3, encodes a putative chloroplast translation elongation factor that is important for chloroplast development in the cold. *BMC Plant Biol* 10: 287

Pubmed: [Author and Title](#)

CrossRef: [Author and Title](#)

Google Scholar: [Author Only](#) [Title Only](#) [Author and Title](#)

Liu X, Zheng M, Wang R, Wang R, An L, Rodermeil SR, Yu F (2013) Genetic interactions reveal that specific defects of chloroplast translation are associated with the suppression of var2-mediated leaf variegation. *J Integr Plant Biol* 55: 979-993

Pubmed: [Author and Title](#)

CrossRef: [Author and Title](#)

Google Scholar: [Author Only](#) [Title Only](#) [Author and Title](#)

Lomakin IB, Shirokikh NE, Yusupov MM, Hellen CU, Pestova TV (2006) The fidelity of translation initiation: reciprocal activities of eIF1, IF3 and YciH. *EMBO J* 25: 196-210

Pubmed: [Author and Title](#)

CrossRef: [Author and Title](#)

Google Scholar: [Author Only](#) [Title Only](#) [Author and Title](#)

Lukowitz W, Gillmor CS, Scheible WR (2000) Positional cloning in Arabidopsis: why it feels good to have a genome initiative working for you. Plant Physiol 123: 795-805

Pubmed: [Author and Title](#)
CrossRef: [Author and Title](#)
Google Scholar: [Author Only](#) [Title Only](#) [Author and Title](#)

Mandel MA, Feldmann KA, Herrera-Estrella L, Rocha-Sosa M, León P (1996) CLA1, a novel gene required for chloroplast development, is highly conserved in evolution. Plant J 9: 649-658

Pubmed: [Author and Title](#)
CrossRef: [Author and Title](#)
Google Scholar: [Author Only](#) [Title Only](#) [Author and Title](#)

Milon P, Konevega AL, Gualerzi CO, Rodnina MV (2008) Kinetic checkpoint at a late step in translation initiation. Mol Cell 30: 712-720

Pubmed: [Author and Title](#)
CrossRef: [Author and Title](#)
Google Scholar: [Author Only](#) [Title Only](#) [Author and Title](#)

Miura E, Kato Y, Matsushima R, Albrecht V, Laalami S, Sakamoto W (2007) The balance between protein synthesis and degradation in chloroplasts determines leaf variegation in Arabidopsis yellow variegated mutants. Plant Cell 19: 1313-1328

Pubmed: [Author and Title](#)
CrossRef: [Author and Title](#)
Google Scholar: [Author Only](#) [Title Only](#) [Author and Title](#)

Mochizuki N, Tanaka R, Tanaka A, Masuda T, Nagatani A (2008) The steady-state level of Mg-protoporphyrin IX is not a determinant of plastid-to-nucleus signaling in Arabidopsis. Proc Natl Acad Sci USA 105: 15184-15189

Pubmed: [Author and Title](#)
CrossRef: [Author and Title](#)
Google Scholar: [Author Only](#) [Title Only](#) [Author and Title](#)

Moulin M, McCormac AC, Terry MJ, Smith AG (2008) Tetrapyrrole profiling in Arabidopsis seedlings reveals that retrograde plastid nuclear signaling is not due to Mg-protoporphyrin IX accumulation. Proc Natl Acad Sci USA 105: 15178-15183

Pubmed: [Author and Title](#)
CrossRef: [Author and Title](#)
Google Scholar: [Author Only](#) [Title Only](#) [Author and Title](#)

Nesbit AD, Whippo C, Hangarter RP, Kehoe DM (2015) Translation initiation factor 3 families: what are their roles in regulating cyanobacterial and chloroplast gene expression? Photosynth Res 126: 147-159

Pubmed: [Author and Title](#)
CrossRef: [Author and Title](#)
Google Scholar: [Author Only](#) [Title Only](#) [Author and Title](#)

Nikovics K, Blein T, Peaucelle A, Ishida T, Morin H, Aida M, Laufs P (2006) The balance between the MIR164A and CUC2 genes controls leaf margin serration in Arabidopsis. Plant Cell 18: 2929-2945

Pubmed: [Author and Title](#)
CrossRef: [Author and Title](#)
Google Scholar: [Author Only](#) [Title Only](#) [Author and Title](#)

Nott A, Jung HS, Koussevitzky S, Chory J (2006) Plastid-to-nucleus retrograde signaling. Annu Rev Plant Biol 57: 739-759

Pubmed: [Author and Title](#)
CrossRef: [Author and Title](#)
Google Scholar: [Author Only](#) [Title Only](#) [Author and Title](#)

Pesaresi P, Hertle A, Pribil M, Kleine T, Wagner R, Strissel H, Ilnatowicz A, Bonardi V, Scharfenberg M, Schneider A, Pfannschmidt T, Leister D (2009) Arabidopsis STN7 kinase provides a link between short- and long-term photosynthetic acclimation. Plant Cell 21: 2402-2423

Pubmed: [Author and Title](#)
CrossRef: [Author and Title](#)
Google Scholar: [Author Only](#) [Title Only](#) [Author and Title](#)

Pesaresi P, Masiero S, Eubel H, Braun HP, Bhushan S, Glaser E, Salamini F, Leister D (2006) Nuclear photosynthetic gene expression is synergistically modulated by rates of protein synthesis in chloroplasts and mitochondria. Plant Cell 18: 970-991

Pubmed: [Author and Title](#)
CrossRef: [Author and Title](#)
Google Scholar: [Author Only](#) [Title Only](#) [Author and Title](#)

Putarjunan A, Liu X, Nolan T, Yu F, Rodermeil S (2013) Understanding chloroplast biogenesis using second-site suppressors of immutans and var2. Photosynth Res 116: 437-453

Pubmed: [Author and Title](#)
CrossRef: [Author and Title](#)
Google Scholar: [Author Only](#) [Title Only](#) [Author and Title](#)

Qi Y, Zhao J, An R, Zhang J, Liang S, Shao J, Liu X, An L, Yu F (2015) Mutations in circularly permuted GTPase family genes AtNOA1/RIF1/SVR10 and BPG2 suppress var2-mediated leaf variegation in Arabidopsis thaliana. Photosynth Res DOI: 10.1007/s11120-015-0195-9

Pubmed: [Author and Title](#)
CrossRef: [Author and Title](#)
Google Scholar: [Author Only](#) [Title Only](#) [Author and Title](#)

Ramel F, Birtic S, Ginies C, Soubigou-Taconnat L, Triantaphyllidis C, Havaux M (2012) Carotenoid oxidation products are stress

signals that mediate gene responses to single to oxygen in plants. *Proc Natl Acad Sci USA* 109: 5535-5540

Pubmed: [Author and Title](#)

CrossRef: [Author and Title](#)

Google Scholar: [Author Only](#) [Title Only](#) [Author and Title](#)

Reiter RS, Coomber SA, Bourett TM, Bartley GE, Scolnik PA (1994) Control of leaf and chloroplast development by the Arabidopsis gene pale cress. *Plant Cell* 6: 1253-1264

Pubmed: [Author and Title](#)

CrossRef: [Author and Title](#)

Google Scholar: [Author Only](#) [Title Only](#) [Author and Title](#)

Royer DL, McElwain JC, Adams JM, Wilf P (2008) Sensitivity of leaf size and shape to climate within *Acer rubrum* and *Quercus kelloggii*. *New Phytol* 179: 808-817

Pubmed: [Author and Title](#)

CrossRef: [Author and Title](#)

Google Scholar: [Author Only](#) [Title Only](#) [Author and Title](#)

Sacerdot C, Fayat G, Dessen P, Springer M, Plumbridge JA, Grunberg-Manago M, Blanquet S (1982) Sequence of a 1.26-kb DNA fragment containing the structural gene for E.coli initiation factor IF3: presence of an AUU initiator codon. *EMBO J* 1: 311-315

Pubmed: [Author and Title](#)

CrossRef: [Author and Title](#)

Google Scholar: [Author Only](#) [Title Only](#) [Author and Title](#)

Saini G, Meskauskiene R, Pijacka W, Roszak P, Sjögren LL, Clarke AK, Straus M, Apel K (2011) 'happy on norflurazon' (hon) mutations implicate perturbation of plastid homeostasis with activating stress acclimatization and changing nuclear gene expression in norflurazon-treated seedlings. *Plant J* 65: 690-702

Pubmed: [Author and Title](#)

CrossRef: [Author and Title](#)

Google Scholar: [Author Only](#) [Title Only](#) [Author and Title](#)

Scarpella E, Marcos D, Friml J, Berleth T (2006) Control of leaf vascular patterning by polar auxin transport. *Genes Dev* 20: 1012-1027

Pubmed: [Author and Title](#)

CrossRef: [Author and Title](#)

Google Scholar: [Author Only](#) [Title Only](#) [Author and Title](#)

Sieburth LE (1999) Auxin is required for leaf vein pattern in Arabidopsis. *Plant Physiol* 121: 1179-1190

Pubmed: [Author and Title](#)

CrossRef: [Author and Title](#)

Google Scholar: [Author Only](#) [Title Only](#) [Author and Title](#)

Sun X, Feng P, Xu X, Guo H, Ma J, Chi W, Lin R, Lu C, Zhang L (2011) A chloroplast envelope-bound PHD transcription factor mediates chloroplast signals to the nucleus. *Nat Commun* 2: 477

Pubmed: [Author and Title](#)

CrossRef: [Author and Title](#)

Google Scholar: [Author Only](#) [Title Only](#) [Author and Title](#)

Susek RE, Ausubel FM, Chory J (1993) Signal transduction mutants of Arabidopsis uncouple nuclear CAB and RBCS gene expression from chloroplast development. *Cell* 74: 787-799

Pubmed: [Author and Title](#)

CrossRef: [Author and Title](#)

Google Scholar: [Author Only](#) [Title Only](#) [Author and Title](#)

Tiller N, Bock R (2014) The translational apparatus of plastids and its role in plant development. *Mol Plant* 7: 1105-1120

Pubmed: [Author and Title](#)

CrossRef: [Author and Title](#)

Google Scholar: [Author Only](#) [Title Only](#) [Author and Title](#)

Ulmasov T, Murfett J, Hagen G, Guilfoyle TJ (1997) Aux/IAA proteins repress expression of reporter genes containing natural and highly active synthetic auxin response elements. *Plant Cell* 9: 1963-1971

Pubmed: [Author and Title](#)

CrossRef: [Author and Title](#)

Google Scholar: [Author Only](#) [Title Only](#) [Author and Title](#)

Wagner D, Przybyla D, Op den Camp R, Kim C, Landgraf F, Lee KP, Würsch M, Laloi C, Nater M, Hideg E, Apel K. (2004) The genetic basis of singlet oxygen-induced stress responses of Arabidopsis thaliana. *Science* 306: 183-185

Pubmed: [Author and Title](#)

CrossRef: [Author and Title](#)

Google Scholar: [Author Only](#) [Title Only](#) [Author and Title](#)

Wilson PB, Estavillo GM, Field KJ, Pornsiriwong W, Carroll AJ, Howell KA, Woo NS, Lake JA, Smith SM, Harvey Millar A, von Caemmerer S, Pogson BJ (2009) The nucleotidase/phosphatase SAL1 is a negative regulator of drought tolerance in Arabidopsis. *Plant J* 58: 299-317

Pubmed: [Author and Title](#)

CrossRef: [Author and Title](#)

Google Scholar: [Author Only](#) [Title Only](#) [Author and Title](#)

Woodson JD, Chory J (2008) Coordination of gene expression between organellar and nuclear genomes. *Nat Rev Genet* 9: 383-395

Pubmed: [Author and Title](#)

CrossRef: [Author and Title](#)

Google Scholar: [Author Only](#) [Title Only](#) [Author and Title](#)

Woodson JD, Chory J (2012) Organelle signaling: how stressed chloroplasts communicate with the nucleus. *Curr Biol* 22: R690-R692

Pubmed: [Author and Title](#)

CrossRef: [Author and Title](#)

Google Scholar: [Author Only](#) [Title Only](#) [Author and Title](#)

Xiang C, Han P, Lutziger I, Wang K, Oliver DJ (1999) A mini binary vector series for plant transformation. *Plant Mol Biol* 40: 711-717

Pubmed: [Author and Title](#)

CrossRef: [Author and Title](#)

Google Scholar: [Author Only](#) [Title Only](#) [Author and Title](#)

Xiao Y, Savchenko T, Baidoo EE, Chehab WE, Hayden DM, Tolstikov V, Corwin JA, Kliebenstein DJ, Keasling JD, Dehesh K (2012) Retrograde signaling by the plastidial metabolite MEcPP regulates expression of nuclear stress-response genes. *Cell* 149: 1525-1535

Pubmed: [Author and Title](#)

CrossRef: [Author and Title](#)

Google Scholar: [Author Only](#) [Title Only](#) [Author and Title](#)

Yoo SD, Cho YH, Sheen J (2007) Arabidopsis mesophyll protoplasts: a versatile cell system for transient gene expression analysis. *Nat Protoc* 2: 1565-1572

Pubmed: [Author and Title](#)

CrossRef: [Author and Title](#)

Google Scholar: [Author Only](#) [Title Only](#) [Author and Title](#)

Yu F, Liu X, Alsheikh M, Park S, Rodermei S (2008) Mutations in SUPPRESSOR OF VARIATION1, a factor required for normal chloroplast translation, suppress var2-mediated leaf variegation in Arabidopsis. *Plant Cell* 20: 1786-1804

Pubmed: [Author and Title](#)

CrossRef: [Author and Title](#)

Google Scholar: [Author Only](#) [Title Only](#) [Author and Title](#)

Yu F, Park S, Rodermei SR (2004) The Arabidopsis FtsH metalloprotease gene family: interchangeability of subunits in chloroplast oligomeric complexes. *Plant J* 37: 864-876

Pubmed: [Author and Title](#)

CrossRef: [Author and Title](#)

Google Scholar: [Author Only](#) [Title Only](#) [Author and Title](#)

Yu F, Park S, Rodermei SR (2005) Functional redundancy of AtFtsH metalloproteases in thylakoid membrane complexes. *Plant Physiol* 138: 1957-1966

Pubmed: [Author and Title](#)

CrossRef: [Author and Title](#)

Google Scholar: [Author Only](#) [Title Only](#) [Author and Title](#)

Yu F, Park SS, Liu X, Foudree A, Fu A, Powikrowska M, Khrouchtchova A, Jensen PE, Kriger JN, Gray GR, Rodermei SR (2011) SUPPRESSOR OF VARIATION4, a new var2 suppressor locus, encodes a pioneer protein that is required for chloroplast biogenesis. *Mol Plant*

Pubmed: [Author and Title](#)

CrossRef: [Author and Title](#)

Google Scholar: [Author Only](#) [Title Only](#) [Author and Title](#)